AMERICAN SOCIETY FOR MICROBIOLOGY | Journal of Bacteriology®

RESEARCH ARTICLE

Distinct Regulatory Role of Carbon Catabolite Protein A (CcpA) in Oral Streptococcal *spxB* Expression

Sylvio Redanz,[a] Revathi Masilamani,[b] Nyssa Cullin,[a,b] Rodrigo A. Giacaman,[c] Justin Merritt,[a] Jens Kreth[a]

[a]Department of Restorative Dentistry, Oregon Health and Science University, Portland, Oregon, USA

[b]Department of Microbiology and Immunology, University of Oklahoma Health Sciences Center, Oklahoma City, Oklahoma, USA

[c]Cariology Unit, Department of Oral Rehabilitation and Interdisciplinary Excellence Research Program on Healthy Aging (PIEI-ES), University of Talca, Talca, Chile

ABSTRACT Pyruvate oxidase (SpxB)-dependent H_2O_2 production is under the control of carbon catabolite protein A (CcpA) in the oral species *Streptococcus sanguinis* and *Streptococcus gordonii*. Interestingly, both species react differently to the presence of the preferred carbohydrate source glucose. *S. gordonii* CcpA-dependent regulation of *spxB* follows classical carbon catabolite repression. Conversely, *spxB* expression in *S. sanguinis* is not influenced by glucose but is repressed by CcpA. Here, we constructed strains expressing the heterologous versions of CcpA or the *spxB* promoter region to learn if the distinct regulation of *spxB* expression is transferable from *S. gordonii* to *S. sanguinis* and vice versa. While cross-species binding of CcpA to the *spxB* promoter is conserved *in vitro*, we were unable to swap the species-specific regulation. This suggests that a regulatory mechanism upstream of CcpA most likely is responsible for the observed difference in *spxB* expression. Moreover, the overall ecological significance of differential *spxB* regulation in the presence of various glucose concentrations was tested with additional oral streptococcus isolates and demonstrated that carbohydrate-dependent and carbohydrate-independent mechanisms exist to control expression of *spxB* in the oral biofilm. Overall, our data demonstrate the unexpected finding that metabolic pathways between two closely related oral streptococcal species can be regulated differently despite an exceptionally high DNA sequence identity.

IMPORTANCE Polymicrobial diseases are the result of interactions among the residential microbes, which can lead to a dysbiotic community. *Streptococcus sanguinis* and *Streptococcus gordonii* are considered commensal species that are present in the healthy dental biofilm. Both species are able to produce significant amounts of H_2O_2 via the enzymatic action of the pyruvate oxidase SpxB. H_2O_2 is able to inhibit species associated with oral diseases. SpxB and its gene-regulatory elements present in both species are highly conserved. Nonetheless, a differential response to the presence of glucose was observed. Here, we investigate the mechanisms that lead to this differential response. Detailed knowledge of the regulatory mechanisms will aid in a better understanding of oral disease development and how to prevent dysbiosis.

KEYWORDS CcpA, hydrogen peroxide, oral biofilm, streptococcus

Next-generation sequencing technologies have recently guided a revision of the etiology of both caries and periodontal diseases based on a better-defined species composition and deeper understanding of oral microbial ecology (1–6). Both oral diseases have a polymicrobial etiology. Polymicrobial diseases are driven by the synergistic and antagonistic interactions among the residential microbial flora. Under the

Received 13 October 2017 **Accepted** 12 January 2018

Accepted manuscript posted online 29 January 2018

Citation Redanz S, Masilamani R, Cullin N, Giacaman RA, Merritt J, Kreth J. 2018. Distinct regulatory role of carbon catabolite protein A (CcpA) in oral streptococcal *spxB* expression. J Bacteriol 200:e00619-17. https://doi.org/10.1128/JB.00619-17.

Editor Tina M. Henkin, Ohio State University

Address correspondence to Sylvio Redanz, redanz@ohsu.edu, or Jens Kreth, kreth@ohsu.edu.

S.R. and R.M. contributed equally.

appropriate environmental conditions, these interactions can favor a shift in the microbial profile and an increased abundance of disease-associated species, referred to as dysbiosis (7, 8). Analysis of metagenomic data also suggests that specific metabolic pathways and genes are associated with caries and periodontal disease and that a functional (metabolic) output of the oral microbial community is more important in disease etiology than a specific taxonomic composition (2, 9). Consequently, understanding specific ecological and molecular processes regulating the functional output of the polymicrobial community during health and disease is of utmost importance.

Streptococci are among the most abundant species found in the early oral biofilm (10, 11), and two prominent members of this polymicrobial community are *Streptococcus sanguinis* and *Streptococcus gordonii*. Both are frequently isolated from healthy and diseased sites. For example, *S. sanguinis* seems to be strongly associated with periodontal health (12), while its abundance is increased significantly in dentin cavities (13). However, this is in sharp contrast to earlier reports showing that *S. sanguinis* is associated with sound enamel (14) and caries-free children (15) and adults (16), indicating that the role of *S. sanguinis* in disease development is not well understood. Similarly, the role of *S. gordonii* in dental biofilm is obscure. Like *S. sanguinis*, *S. gordonii* is an early colonizer of dental surfaces, providing attachment sites for successive recruitment of other oral microbial species (17, 18). Under normal conditions, the recruitment would lead to the development of a healthy dental biofilm synergistic with the host. On the other hand, several studies have shown that *S. gordonii* is able to interact with and support certain periodontal pathogens. Heterotypic community development with *Porphyromonas gingivalis* might be orchestrated by metabolic cross feeding and interspecies signaling events (19–22). Furthermore, association of *S. gordonii* with *Aggregatibacter actinomycetemcomitans* establishes a beneficial environment for *A. actinomycetemcomitans* to survive host innate immunity (23). A central role in this relationship is *S. gordonii*'s ability to produce hydrogen peroxide (H_2O_2), which induces *katA* and *apiA* gene expression in coculture of both species. KatA is a cytoplasmic catalase that might aid in detoxification of H_2O_2 produced during a neutrophil attack. ApiA is able to inhibit complement-dependent killing by binding human serum protein factor H (23).

Production of H_2O_2 is not restricted to *S. gordonii*. H_2O_2 is the metabolic by-product of acetyl-phosphate generation by the oxidoreductase pyruvate oxidase SpxB. Surprisingly, the *spxB* gene has a remarkable degree of conservation among oral streptococci (24, 25). The importance of H_2O_2 production by *S. sanguinis* and *S. gordonii* has been demonstrated *in vitro* mainly in the interspecies interaction with H_2O_2-susceptible *Streptococcus mutans* (26, 27) and *Actinomyces* (28), both frequently isolated from caries active sites (29, 30). Besides the inhibitory H_2O_2 action, SpxB activity is associated with two other metabolically and ecologically relevant activities: (i) ATP production from acetyl-phosphate for metabolic energy generation and (ii) release of extracellular DNA (eDNA), promoting biofilm formation, cell-cell aggregation, and cell-tooth adhesion (24). Furthermore, *spxB* is expressed in oral plaque samples (25), suggesting an important ecological role of SpxB in the dental biofilm, possibly contributing to a functional (metabolic) output of the oral microbial community due to its abundant distribution among oral streptococci.

The relatively wide distribution and conservation of the *spxB* gene among oral streptococci raises interest about the molecular mechanisms involved in expression regulation. It was previously established that several environmental factors, including oxygen and carbohydrate availability, influence *spxB* expression in *S. sanguinis* and *S. gordonii* (31, 32). In addition, the central carbon catabolite regulator CcpA (for catabolite control protein A) plays a major role in the regulation of *spxB* expression (33, 34). While the predicted binding of CcpA to the *S. gordonii spxB* promoter was confirmed *in vitro* (31) and mutational studies support CcpA-dependent regulation of *spxB* in *S. sanguinis* (35), one key difference remained unresolved. In *S. gordonii*, CcpA-dependent regulation of *spxB* followed the classical carbon catabolite repression model (31) with glucose repressing *spxB* expression. In contrast, *spxB* expression in *S. sanguinis* was not influenced by any carbohydrate source (35).

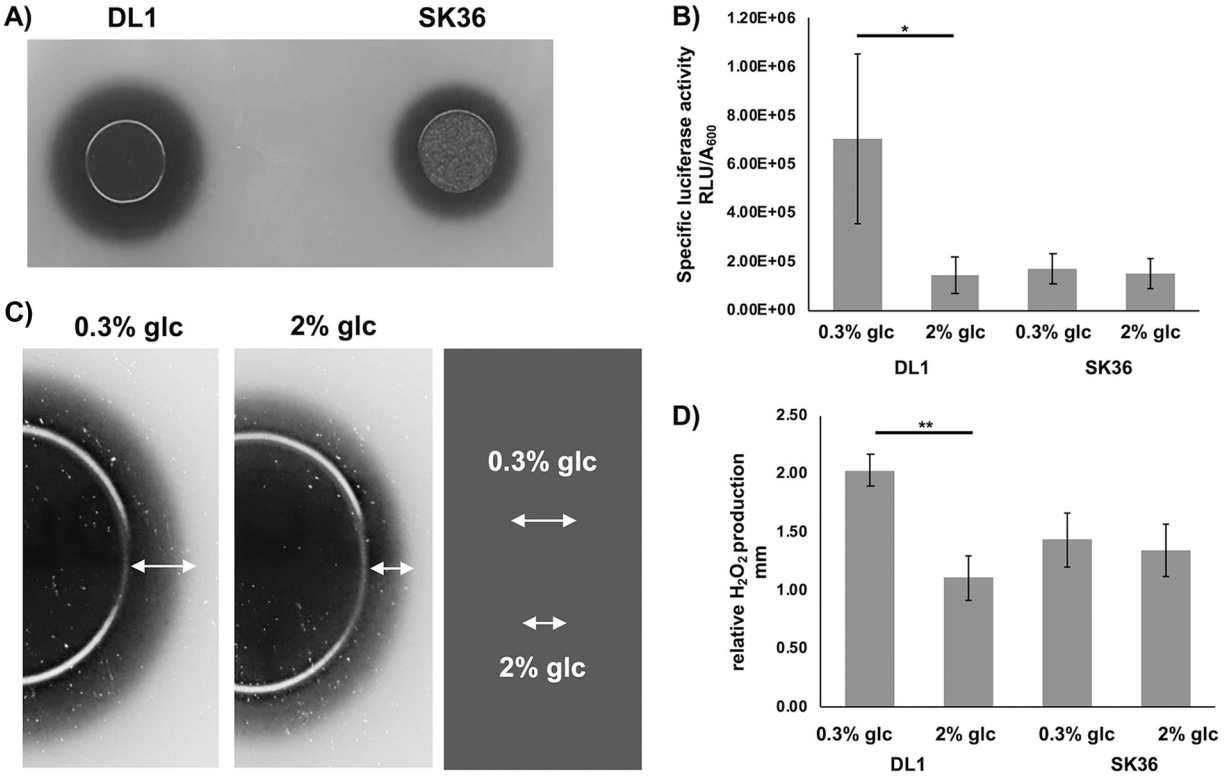

FIG 1 Differential *spxB* expression and H_2O_2 production by *S. sanguinis* SK36 and *S. gordonii* DL1. (A) H_2O_2 production of *S. sanguinis* SK36 and *S. gordonii* DL1 on H_2O_2 indicator plates after overnight incubation. H_2O_2 production leads to the precipitation of Prussian blue during aerobic growth. Shown is a representative picture of two independent experiments. (B) Specific luciferase activity of *S. sanguinis* and *S. gordonii* cells grown aerobically with 0.3% or 2% glucose; presented are averages and standard deviations ($n = 5$). (C) Illustration of how the production of H_2O_2 was assessed. Presented as an example is *S. gordonii* grown in the presence of 0.3% or 2% glucose. The distance between the edge of the colony and the end of the precipitation zone was determined as a measure of relative H_2O_2 production. (D) Relative H_2O_2 production of *S. sanguinis* SK36 and *S. gordonii* DL1 cells grown aerobically on H_2O_2 indicator agar plates with 0.3% and 2% glucose (glc). Presented are averages and standard deviations from at least five independent experiments. Significant differences are indicated by asterisks (paired, two-tailed *t* test; *, $P < 0.05$; **, $P < 0.01$).

In this study, we aimed to understand the molecular basis of this differential regulation of *spxB* gene expression. Using *in vitro* binding studies with electromobility shift assays (EMSA), we show that CcpA binds to the *spxB* promoter in *S. sanguinis*. With the help of strains expressing the heterologous version of CcpA or the *spxB* promoter region, we examined if the distinct regulation of *spxB* expression is transferable between species. In addition, we examined SpxB-dependent H_2O_2 production in response to glucose with several oral streptococcal isolates, demonstrating that differential *spxB* expression regulation is present in the dental biofilm. Overall, our study provides important insight into species-specific regulation of *spxB* expression and suggests that the functional (metabolic) output of the oral microbial community determines oral health and disease, but species-specific regulation of this functional output requires careful investigation.

RESULTS

Effect of glucose on carbon catabolite repression of *spxB* expression and H_2O_2 production. To determine H_2O_2 production, an agar plate indicator assay based on the production of Prussian blue, which precipitates in the presence of H_2O_2, was used (36). *S. sanguinis* and *S. gordonii* are H_2O_2 producers under aerobic conditions with a significant difference in the amount of H_2O_2 secreted into the environment (Fig. 1A). Deletion of CcpA in both *S. sanguinis* and *S. gordonii* abolished the carbon catabolite-dependent repression of *spxB* (31, 35). To directly compare the effect of low (0.3%) and high (2%) glucose concentrations on *S. gordonii* and *S. sanguinis* H_2O_2 production, luciferase reporter assays were performed (Fig. 1B). Expression of *spxB* is strongly

influenced by oxygen tension (27); therefore, cells were grown aerobically in liquid brain heart infusion (BHI) under vigorous shaking to maximize oxygen exposure as reported before (27, 35). *S. gordonii* did show a 4-fold reduction in luciferase activity when grown in the presence of 2% glucose. Conversely, *S. sanguinis* did not respond with a decrease in *spxB* expression when grown in the presence of 2% glucose. Compared to *S. gordonii*, *S. sanguinis* appeared to repress *spxB* expression more tightly, independent of the carbohydrate concentration (Fig. 1B). Previously, we showed that galactose strongly repressed *spxB* expression in *S. gordonii* (31). To learn if the observed repressed *spxB* expression in *S. sanguinis* is independent of the carbohydrate source, we also measured the production of H_2O_2 in the presence of galactose and sucrose. No differences were observed between high and low carbohydrate concentrations, suggesting that the repression of *spxB* expression in *S. sanguinis* is carbohydrate independent for the tested carbohydrate sources (data not presented).

To confirm that the observed carbon catabolite repression in *S. gordonii* and the tight repression of *spxB* in *S. sanguinis* are accompanied by similar H_2O_2 production phenotypes, cells were grown on H_2O_2 indicator plates. Relative H_2O_2 production was quantified by measuring the distance between the edge of the colony and the edge of the blue halo (Fig. 1C, shown for *S. gordonii*) formed after 16 h of incubation. Production of H_2O_2 followed *spxB* gene expression patterns (Fig. 1D) observed for both species. Overall, these results support a differential regulation of *spxB* expression in *S. sanguinis* and *S. gordonii* by CcpA. *S. gordonii* follows the classic carbon catabolite repression model, while *S. sanguinis* seems to repress *spxB* by a carbohydrate-independent mechanism.

CcpA binds to the *S. sanguinis spxB* promoter. The differential regulation of *spxB* expression in *S. sanguinis* and *S. gordonii* was surprising, since the alignment of the promoter regions of both species only showed minimal nucleotide changes (Fig. 2A). The *in silico* analysis for the presence of *cre* (carbon-responsive element) sites for CcpA binding (33) predicted two binding sites in the *S. gordonii spxB* promoter, designated *cre* 1 and *cre* 2 (as shown in Fig. 2A). We verified the *in silico*-predicted presence of two *cre* sites for *S. gordonii* by mutational analysis earlier (31). However, there was only one predicted site for *S. sanguinis* $spxB_p$, designated *cre* 1. Interestingly, there was one nucleotide exchange in the region aligning with *S. gordonii cre* 2, suggesting the existence of a *cre* 2 site (Fig. 2A, highlighted in italics in the *S. sanguinis* sequence). To confirm binding of CcpA to the *spxB* promoter of *S. sanguinis*, CcpA was engineered to carry a C-terminal His_6 tag for protein overexpression in *E. coli* and Ni affinity purification. The protein was successfully purified and used for EMSA. A biotin-labeled 200-bp PCR-generated $spxB_p$ fragment, amplified from SK36 chromosomal DNA carrying the intact *cre*, was used as the template for binding. Initially 20, 40, and 80 pmol purified CcpA was used for the binding studies, showing a band shift of the respective probe (data not shown). Based on this result, a set of experiments was performed with 20 pmol CcpA. While binding to the $spxB_p$ probe caused a complete shift, no shift was observed with the unrelated $niaX_p$ not encoding a *cre* site (Fig. 2B). In addition, deletion of the region encoding the predicted *cre* 1 site did interfere with binding, only showing a faint band at the expected size of the protein-DNA complex. Interestingly, deletion of *cre* 2 affected CcpA binding as well, but it was not as pronounced as that with deletion of *cre* 1. As expected, deletion of *cre* 1 and *cre* 2 abolished CcpA binding, while engineering both *cre* sites into $niaX_p$ resulted in a shift, albeit not a complete one (Fig. 2C). Overall the results confirm the importance of both *cre* sites for CcpA binding. We did, however, recognize that the engineered promoter regions caused extra bands to appear which might be due to the usage of probes amplified from gBlock gene fragments as the PCR template.

The binding specificity of CcpA to the *S. sanguinis spxB* promoter was further confirmed with a competition assay using unlabeled DNA. A CcpA concentration of 20 pmol was used with 1 fmol biotin-labeled *spxB* promoter sequence. Addition of a 100-fold excess of unlabeled competitor DNA led to the appearance of unbound probe

A)

```
DL1  spxBp   ------GGGATTGAGCATCTCTGAGCATATTCTTATACAAGTGAGAAAAAACATGGTAAA
SK36 spxBp   GTAATAGTTCTATATCATCTTTGAGCATATTCTTATACAAGAGCGAAAAAACATGATAAA
             *   *  * ***** ******************** * *********** ****
                                    cre 1                cre 2
DL1  spxBp   TTGATATAGTAAAGTTTCTTGAAGCGTTTTCATTCACAAATGGAAATGTTTTCAATAACT
SK36 spxBp   TTGATAGAGTAAAGTTTCTTGAAGCGTTTTCATTCACAAATGGAAATATTTTCAACAACT
             ****** ****************************************** ******* ****

DL1  spxBp   GAAAATTTATTTTATTGAAGGAGAGTTATTCTTATG
SK36 spxBp   GAAAATTTATTTTATTGAAGGAGAGTTATT---ATG
             ******************************   ***
```

B)

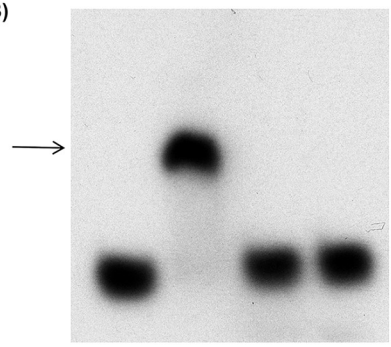

***spxB*$_p$**	+	+		
***niaX*$_p$**			+	+
CcpA		+		+

C)

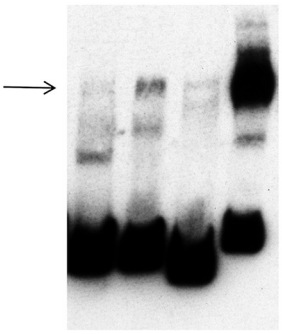

***spxB*$_p$ Δ*cre* 1**	+			
***spxB*$_p$ Δ*cre* 2**		+		
***spxB*$_p$ Δ*cre* 1+2**			+	
***niaX*$_p$::*cre* 1+2**				+
CcpA	+	+	+	+

FIG 2 *spxB* promoter sequence alignment and EMSA analysis of CcpA binding. (A) The sequences of both *spxB* promoters from *S. sanguinis* and *S. gordonii* were aligned, including the ATG start codon (underlined). The boldfaced, underlined sequences depict the predicted *cre* sites as determined by the RegPrecise transcription factor database. (B) EMSA analysis of *S. sanguinis* CcpA with binding substrate *spxB*$_p$. Twenty picomoles of CcpA was incubated with 1 fmol of *spxB*$_p$ substrate. As a negative control, the unrelated *niaX* promoter was used which has no predicted *cre* site. A representative picture is shown ($n = 3$). (C) EMSA with engineered promoter sequences. Twenty picomoles of CcpA was incubated with 1 fmol of substrate. A representative picture of two independent experiments is shown.

with complete disappearance of the shifted band at a 500-fold excess of unlabeled competitor DNA (see Fig. S1 in the supplemental material). In addition, we confirmed the previous EMSA results of CcpA binding to the *S. gordonii spxB* promoter (31; data not shown). This result supports a direct regulatory role of CcpA in *spxB* expression in *S. sanguinis* and *S. gordonii*.

DNA footprinting analysis of CcpA binding to the *S. sanguinis spxB* promoter identifies two *cre* sites. Direct comparison of the *cre* sites between *S. sanguinis* and *S. gordonii* showed 100% conservation of the nucleotide sequence for *cre* 1 and only one mismatch for *cre* 2, yet only one *cre* site was predicted for *S. sanguinis spxB*$_p$ (37). The EMSA results suggest that *spxB*$_p$ from *S. sanguinis* has two functional CcpA binding sites. DNase I footprinting followed by automated capillary electrophoresis (DFACE) was used to investigate the prediction of only a single *cre* site in *S. sanguinis spxB*$_p$. The concentration of CcpA and DNA was identical to that used for EMSA in Fig. 2B. The histograms shown in Fig. 3A and B present relative fluorescence units, which are negative for the predicted *cre* 1 and *cre* 2 sites, indicating protected regions for both binding sites. No protection was observed with the *niaX* promoter (Fig. 3B), strongly suggesting that two functional *cre* sites are present in the *spxB* promoter of *S. sanguinis*.

Differences in the amino acid sequence of CcpA of *S. sanguinis* and *S. gordonii* are localized primarily in the C-terminal domain. Despite the differential regulation of *spxB* expression by CcpA, the alignment of the promoter sequences showed a surprisingly high conservation, which prompted further investigation of the amino acid composition of CcpA itself. Overall, CcpA consists of 334 amino acids in both species, with 27 amino acids being different (Fig. 4). CcpA architecture includes an N-terminal

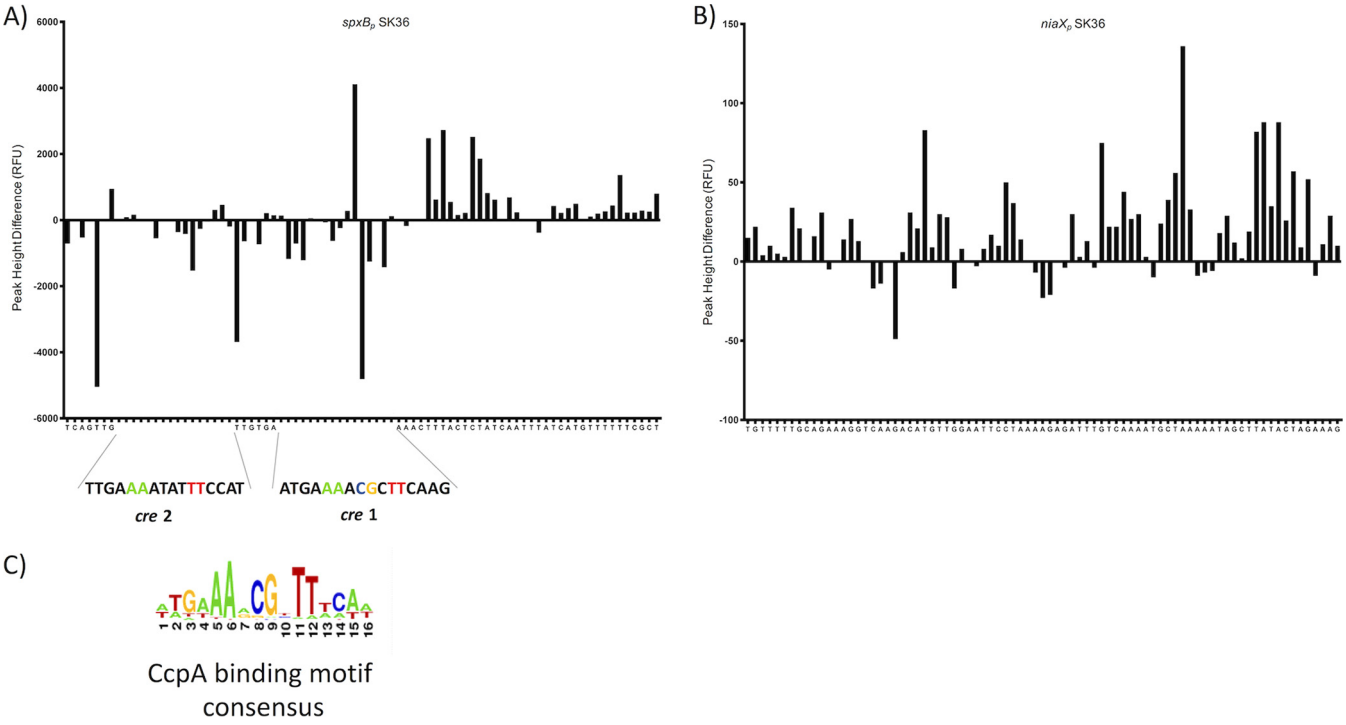

FIG 3 DNase I footprint followed by DFACE analysis to determine CcpA binding. DNase I digestion patterns are shown as histograms of relative fluorescence units (RFU). Negative changes indicate regions of protection, and positive changes indicate hypersensitivity. (A) $spxB_p$. (B) $niaX_p$.

helix-turn-helix (HTH) motif conferring *cre* site recognition via DNA binding and a larger C-terminal domain formed by the PBP-N and PBP-C subdomains, which are named after their resemblance to periplasmic binding proteins (38, 39). The C-terminal domain is responsible for dimerization and effector interaction with other proteins, like the histidine phosphocarrier protein (HPr), a component of the phosphoenolpyruvate-dependent sugar phosphotransferase system (PTS) (39). The sequence alignment of *S. sanguinis* and *S. gordonii* CcpA shows that the majority of amino acid differences are found in the C-terminal part of CcpA, with 26 out of 27 differences, leaving the HTH domain unchanged (Fig. 4).

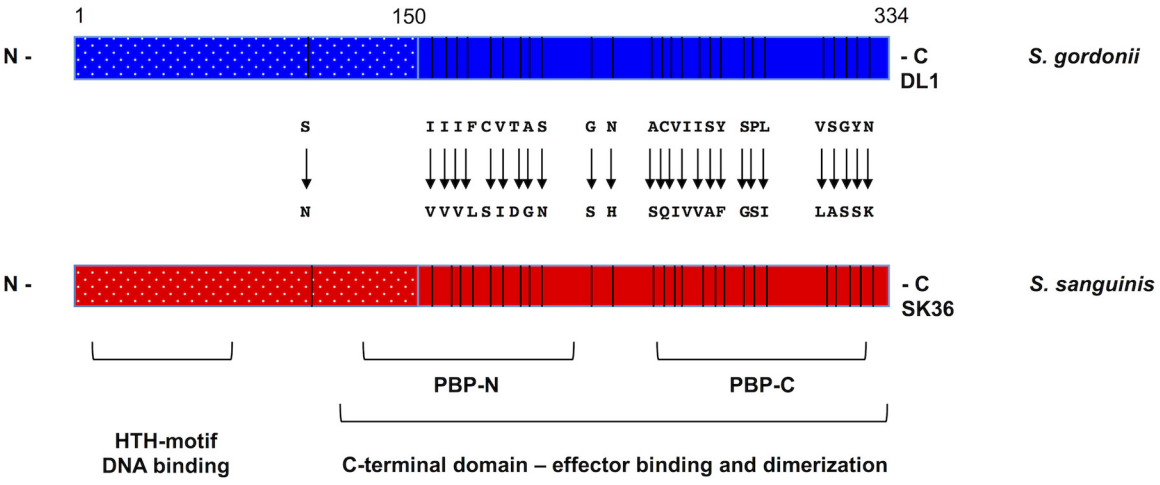

FIG 4 Schematic diagram of CcpA of *S. sanguinis* and *S. gordonii*. Presented are the relative positions of the domain structures for the N-terminal helix-turn-helix (HTH) DNA binding motif and the C-terminal effector binding domain consisting of PBP-N and PBP-C, as well as all amino acid differences between both proteins.

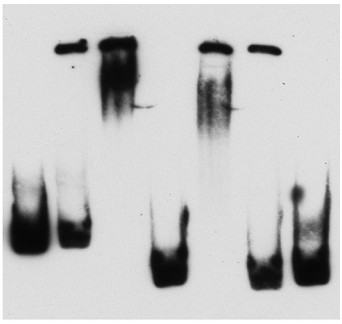

CcpA (DL1)		+	+				
CcpA (SK36)					+	+	+
$spxB_p$ (DL1)	+	+				+	
$spxB_p$ (SK36)			+	+	+		
$niaX_p$ (SK36)							+

FIG 5 Cross-species EMSA analysis of CcpA binding to $spxB_p$. Twenty picomoles of CcpA of *S. sanguinis* or *S. gordonii* was incubated with 1 fmol of $spxB_p$ of *S. sanguinis* or *S. gordonii* substrate in various combinations. SK36 $niaX_p$ served as a negative control. A representative picture is shown ($n = 3$).

Cross-species recognition of *cre* sites by both CcpA proteins *in vitro*. The HTH domain confers recognition and binding to the *cre* site and showed no changes in amino acid sequence when both species were compared; therefore, we hypothesized that *S. gordonii* CcpA is able to recognize the *S. sanguinis spxB* promoter and vice versa. Both CcpA proteins were used at a concentration of 20 pmol with 1 fmol of the respective promoter fragment. As presented in Fig. 5, *S. sanguinis* and *S. gordonii* CcpA were able to recognize and bind to the respective *spxB* promoter sequences of the other species. This result suggests that the overall binding features of CcpA are well conserved between *S. sanguinis* and *S. gordonii*.

Species-specific H_2O_2 production and *spxB* regulation is invariant. After confirming *in vitro* that CcpA is able to recognize heterologous *cre* sites, we next utilized strains of *S. gordonii* and *S. sanguinis* carrying Δ*ccpA* mutations. We complemented the mutations with the respective CcpA of the other species to learn if the regulatory effect of CcpA-dependent control of H_2O_2 production is transferable from one species to the other. As shown in Fig. 6 for *S. gordonii* and in Fig. 7 for *S. sanguinis*, the parental Δ*ccpA* strain did lift repression of H_2O_2 production and rendered H_2O_2 production nonresponsive to glucose, as expected. Interestingly, complementation with the respective CcpA of the other species fully restored the production of H_2O_2 to the species-specific background. This suggests that the cellular context for the overall regulation of H_2O_2 production is more important than CcpA itself and thus the regulatory effect of CcpA-dependent control of H_2O_2 production is not transferable. Furthermore, we studied the effect of the cross-species *spxB* promoter region on H_2O_2 production, replacing the respective *spxB* promoter of *S. sanguinis* with *S. gordonii* and vice versa. As shown in Fig. 6 and 7, the promoter region did not influence the species-specific production of H_2O_2. To confirm the observed effect on H_2O_2 production and exclude any differences in cell density, we also measured luciferase activity of *spxB* reporter strains carrying $spxB_p$-*luc* fusions to their own or heterologous promoter regions with aerated planktonic cultures. As expected, luciferase activity was indistinguishable and followed similar trends for the specific species carrying either the endogenous or heterologous *spxB* promoter (Fig. 8).

Structural modeling of *S. gordonii* and *S. sanguinis* CcpA. The structures of CcpA from *S. sanguinis* and *S. gordonii* were predicted using the I-TASSER algorithm (40), and the solved structure of CcpA from *Bacillus subtilis* (PDB entry 1ZVV) (41) was used as a template (Fig. S2A to C). Predicted β-sheet regions are depicted in green and α-helical regions are depicted in blue. The respective Ramachandran plots for structure valida-

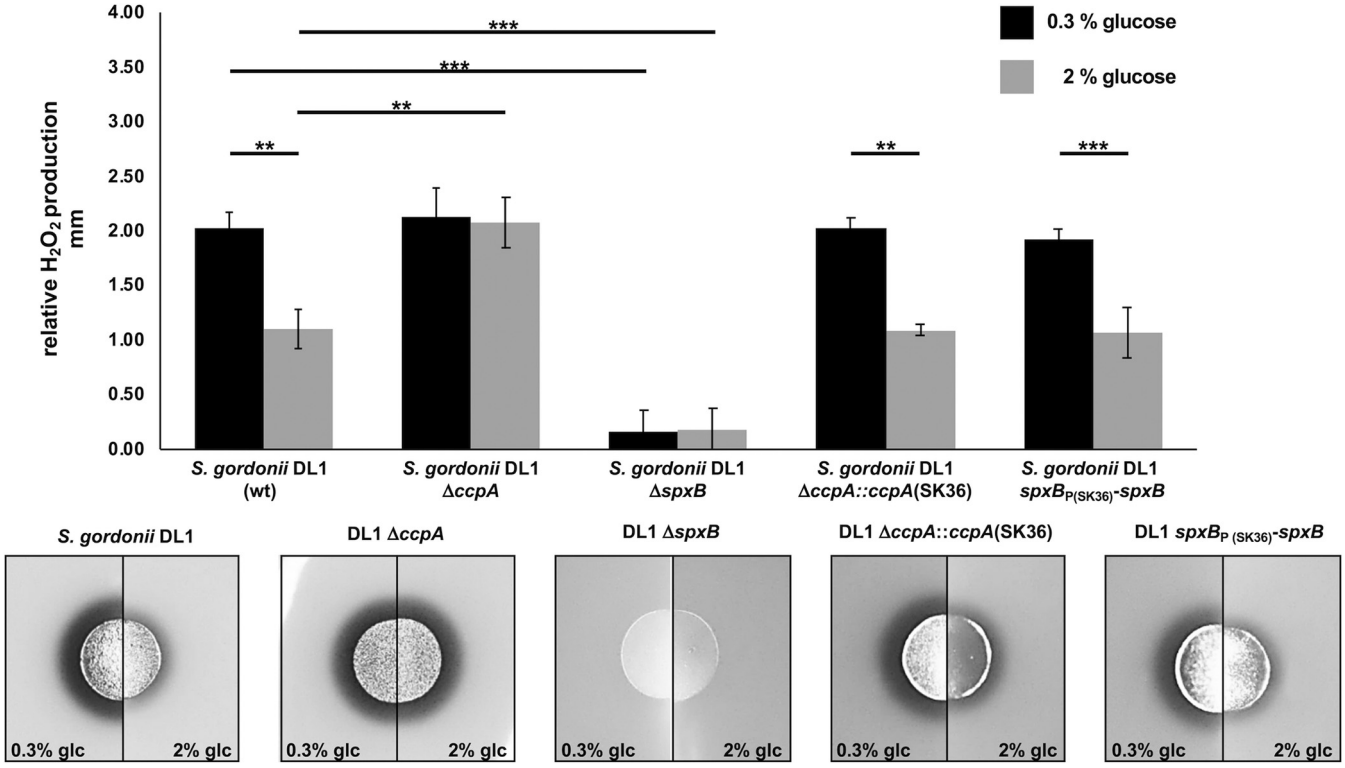

FIG 6 Differential H_2O_2 production of *S. gordonii* DL1 wild-type and mutant strains, shown as relative H_2O_2 release. Cells were grown aerobically on H_2O_2 indicator agar plates with 0.3% and 2% glucose (glc). Presented are averages and standard deviations from at least four independent experiments. Significant differences are indicated by asterisks (two-tailed *t* test; **, $P < 0.01$; ***, $P < 0.001$).

tion are shown in Fig. S3A and B; the plots confirmed the predicted structures with percentages in the most favored regions of 83.3% (SK36) and 86.6% (DL1). Overall the predicted structures resembled each other closely. One major difference was observed in the PBP-C subdomain. Highlighted in yellow is an α-helical region (from amino acid 266 to amino acid 270) in *S. gordonii*, which seems to be a loop in *S. sanguinis* (Fig. S2A and B, arrow). Overall the structural conservation supports the previous results that suggest that the regulatory difference between *S. sanguinis* and *S. gordonii* is upstream of CcpA.

Expression of predicted CcpA-regulated genes in *S. sanguinis* and *S. gordonii* responds differently to increased glucose concentrations. In addition to *spxB*, six genes were selected that have identified *cre* sites in their promoter regions, suggesting CcpA-dependent regulation. Similar to the carbohydrate-independent expression of *spxB* in *S. sanguinis*, the other tested genes also failed to respond with carbon catabolite repression when the concentration of glucose was increased from 0.3% to 2%. Surprisingly, the sucrose-specific PTS system II ABC component encoded by *scrA* even slightly increased in expression at 2% glucose. Interestingly, the effect of increased glucose availability on carbon catabolite repression in *S. gordonii* seemed to be most pronounced for *spxB*, followed by *ccpA* itself and *scrA*, while the other tested genes also showed no difference comparable to what we observed for *S. sanguinis* (Fig. 9).

To investigate this more in detail, experiments were repeated with the *ccpA* deletion mutants of SK36 and DL1. The resulting data indicate a different pattern of CcpA-dependent regulation in SK36 and DL1 (Fig. 10): *manL*, part of the mannose-specific phosphotransferase system, shows highly elevated transcript abundance in SK36 after *ccpA* had been deleted, indicating strong repression by CcpA. In contrast, in DL1 the transcript abundance in the *ccpA* mutant decreased compared to that of the parental wild-type (wt) strain. This indicates that CcpA has a (direct or indirect) function as a transcription activator under the selected conditions. The genes *ldh*, *eno*, and *pykF* were

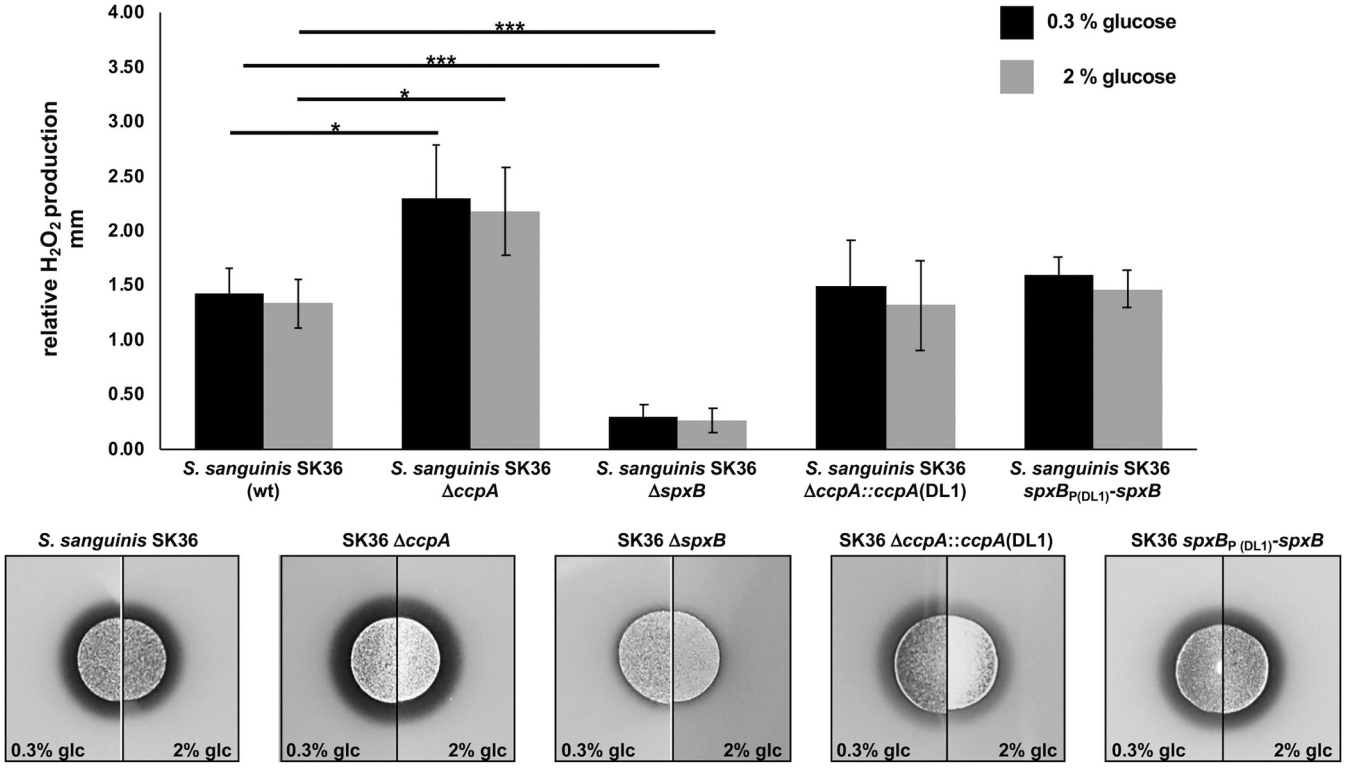

FIG 7 Differential H_2O_2 production of *S. sanguinis* wild-type and mutant strains, shown as relative H_2O_2 release. Cells were grown aerobically on H_2O_2 indicator agar plates with 0.3% and 2% glucose (glc). Presented are averages and standard deviations from at least four independent experiments. Significant differences are indicated by asterisks (two-tailed *t* test; *, $P < 0.05$; ***, $P < 0.001$).

downregulated in the *ccpA* mutants (although not significantly in SK36). Again, CcpA seems to have a more activating function for these genes. *scrA* is clearly under the repression of CcpA in both strains. After deletion of *ccpA*, its transcript abundance increased, significantly in the case of SK36. An opposing regulatory effect of *ccpA* could be ruled out for the *scrA* gene in SK36 and DL1.

Survey of clinical H_2O_2-producing strains from dental plaque samples confirms differential regulation of H_2O_2 production. To learn if the observed differential regulation of *spxB* expression in the presence of carbohydrates is unique to the investigated species, other available oral streptococci from the laboratory collection as well as several clinical isolates from a previous study (25) were tested for H_2O_2 production in the presence of 0.3% and 2% glucose (Fig. 9). The observed response pattern of the additionally tested strains leads to the classification of three groups: I, high-level H_2O_2 production, carbon catabolite repression (CCR) insensitive; II, low-level H_2O_2 production, CCR insensitive; and III, CCR-sensitive H_2O_2 production. Interestingly, the production pattern was not strictly species specific, as several strain-specific responses were observed (Fig. 11). Overall, these results confirm that the production of H_2O_2 is subject to differential regulation in the *in vivo* dental biofilm and not just confined to commonly used and domesticated laboratory strains.

The *spxB* promoter regions of clinical strains do not explain their differential regulation of H_2O_2 production. To identify the reason for the observed differential regulation of H_2O_2 release in the clinical isolates investigated here, we sequenced the *spxB* promoter regions and found a very heterogenic structure even within representatives of the same species. Comparing around 200 nucleotides upstream of the ATG start codon, we identified different lengths of the spacer between the Shine-Dalgarno sequence (5′-AGGAG-3′) (42) and the *spxB* start codon, varying between 7 and 10 nucleotides (Fig. S4). Interestingly, these variations are not linked to any of the above-described groups classifying the regulation-type *spxB* expression and of H_2O_2

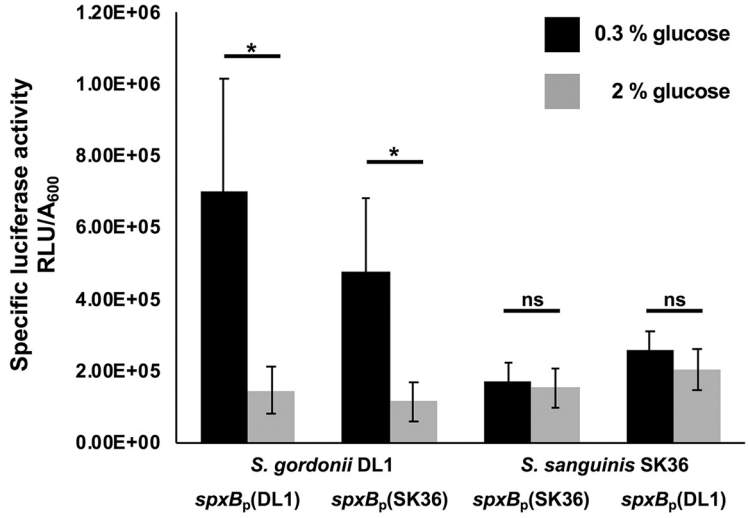

FIG 8 Activity assay of *spxB* in SK36 and DL1. The firefly luciferase gene was fused to the *spxB* promoters of *S. sanguinis* SK36 or *S. gordonii* DL1 and introduced into the two species, resulting in SK36 $spxB_{p(SK36)}$-*luc*/DL1 $spxB_{p(DL1)}$-*luc* with luciferase under the control of the *spxB* promoter of the same species and SK36 $spxB_{p(DL1)}$-*luc*/DL1 $spxB_{p(SK36)}$-*luc* with luciferase under the control of the *spxB* promoter of the other species. Cells were grown overnight in BHI and washed in PBS, and the A_{600} was adjusted to 0.5. Four milliliters of BHI with or without the addition of glucose was inoculated with 350 μl of PBS-washed cells and aerobically incubated (200 rpm, 37°C). After 5 h of incubation, luciferase activity was measured and normalized to the optical density. Each experiment was performed in three technical and five biological replicates. Shown are averages and standard deviations. Significant differences are indicated by asterisks (two-tailed paired *t* test; *, $P < 0.05$; ns, not significant).

production. Further, based on the consensus sequence for *cre* in streptococcaceae (5′-WWGWAARCGYTTWCWW-3′) (Fig. 3C) (43), we found several of these possible CcpA binding sites. The number of predicted *cre* sequences varied between two and three. Again, no connection to one of the above-described groups could be found.

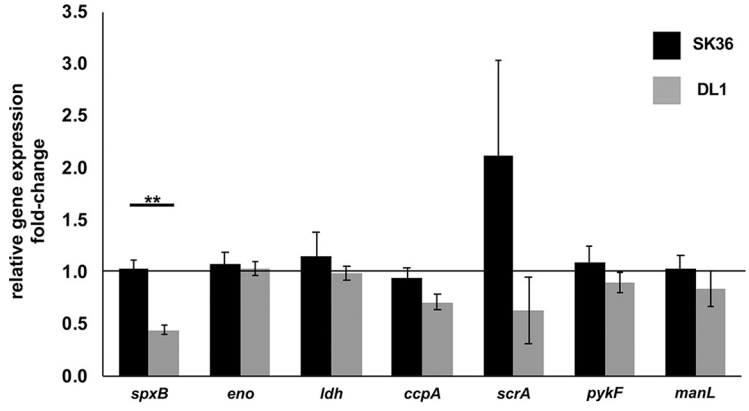

FIG 9 Relative gene expression of putative CcpA-dependent genes. Gene expression is shown as fold change of cells cultured with 2% glucose normalized to growth at 0.3% glucose. Standard deviations are indicated by error bars. *spxB*, pyruvate oxidase (SSA_0391; SGO_0292); *eno*, enolase gene (SSA_0886; SGO_1426); *ldh*, L-lactate dehydrogenase gene (SSA_1221; SGO_1232); *ccpA*, catabolite control protein A gene (SSA_1576; SGO_0773); *scrA*, gene for phosphotransferase system IIC components, glucose/maltose/*N*-acetylglucosamine specific (SSA_0456, SGO_1857); *pykF*, pyruvate kinase gene (SSA_0848; SGO_1339); *manL*, gene for phosphotransferase system, mannose-specific EIIAB (SSA_1918; SGO_1679). Genes were selected based on the RegPrecise transcription factor database (37). Cells were grown overnight in BHI and washed in PBS, and the A_{600} was adjusted to 0.5. Four milliliters of BHI with or without the addition of glucose was inoculated with 350 μl of PBS-washed cells and aerobically incubated (200 rpm, 37°C). After 5 h of incubation, the RNA was isolated and quantitative PCR was performed. All experiments were performed in two technical and three biological replicates. Significant differences are indicated by asterisks (two-tailed paired *t* test; **, $P < 0.01$).

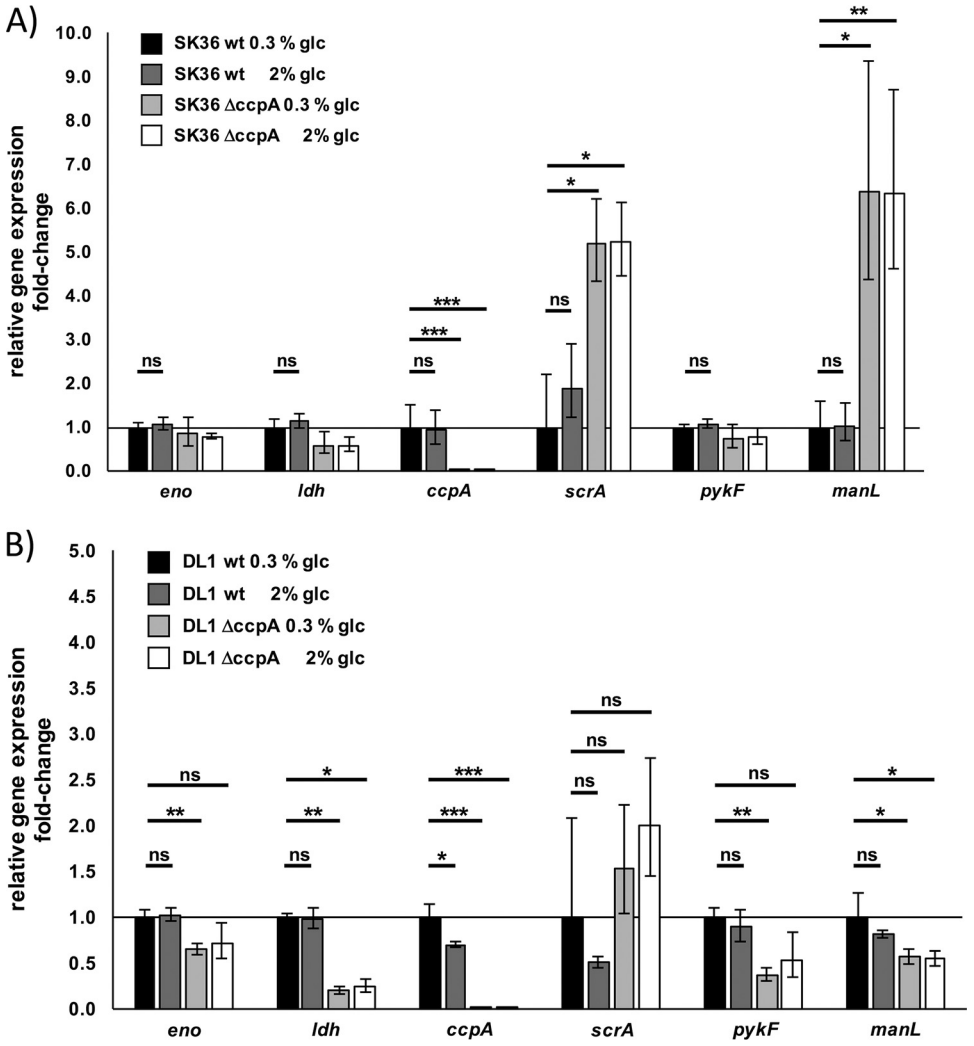

FIG 10 Relative gene expression of various *ccpA*-dependent genes in *S. sanguinis* SK36 (A) and *S. gordonii* DL1 (B) wt and isogenic *ccpA* deletion mutants. Gene expression is shown as fold change of cells cultured with or without the addition of 2% glucose normalized to the growth of the respective wt without the addition of glucose. Standard deviations are indicated by error bars. *eno*, enolase gene (SSA_0886; SGO_1426); *ldh*, L-lactate dehydrogenase gene (SSA_1221; SGO_1232); *ccpA*, catabolite control protein A gene (SSA_1576; SGO_0773); *scrA*, gene for phosphotransferase system IIC components, glucose/maltose/*N*-acetylglucosamine specific (SSA_0456, SGO_1857); *pykF*, pyruvate kinase gene (SSA_0848; SGO_1339); *manL*, gene for phosphotransferase system, mannose-specific EIIAB (SSA_1918; SGO_1679). Genes were selected based on the RegPrecise transcription factor database (37). Cells were grown overnight in BHI and washed in PBS. The OD was adjusted to an A_{600} of 0.5. Four milliliters of BHI with or without the addition of glucose was inoculated with 350 μl of PBS-washed cells and aerobically incubated (200 rpm, 37°C). After 5 h of incubation, the RNA was isolated and quantitative PCR was performed. The shown data represent two technical and three biological replicates. Significant differences are indicated by asterisks (two-tailed *t* test [unpaired]; ns, not significant; *, $P < 0.05$; **, $P < 0.01$; ***, $P < 0.001$).

DISCUSSION

The pyruvate oxidase (SpxB) metabolic pathway leading to the production and subsequent release of H_2O_2 into the environment is highly conserved among the oral streptococcal community, including the numerically abundant *S. sanguinis* and *S. gordonii* (25). Expression of the respective *spxB* gene could be detected in freshly isolated human plaque samples, suggesting at least a metabolic role when the bacteria reside in the dental biofilm (25, 44). The current understanding of disease etiology of polymicrobial dysbiosis such as caries points to the importance of metabolic pathways in disease development, and the functional (metabolic) output of the oral microbial community is more important in disease etiology than a specific taxonomic composition (2). Subsequently, there should also be a metabolic output defining a healthy

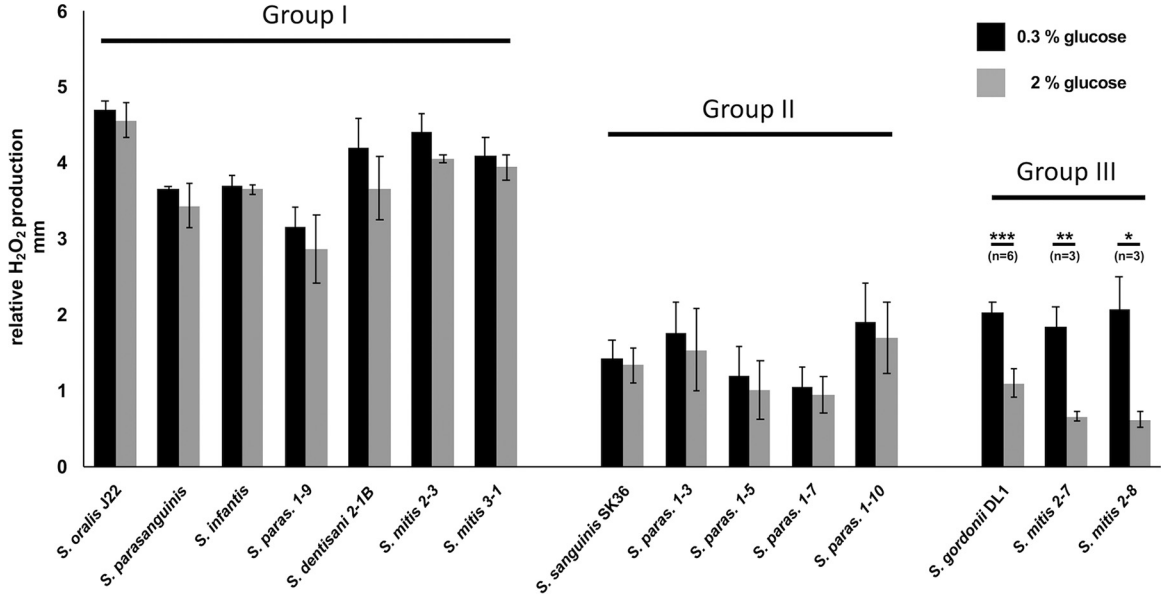

FIG 11 Differential H_2O_2 production of *S. oralis* J22, S. *gordonii* DL1, *S. sanguinis* SK36 (laboratory strains), and several clinical isolates. Shown is the relative H_2O_2 release. Cells were grown aerobically on H_2O_2 indicator agar plates with 0.3% and 2% glucose (glc). Presented are averages and standard deviations from at least three independent experiments. Significant differences are indicated by asterisks (two-tailed *t* test; *, $P < 0.05$; **, $P < 0.01$; ***, $P < 0.001$). The species of clinical isolates were determined by sequencing of the 16S rRNA gene and *recA*. Species were grouped by their amount of H_2O_2 release and their response to the presence of glucose (H_2O_2 release under catabolite control). Group I shows large amounts of H_2O_2 and no or weak response to the presence of glucose. Members of group II release less H_2O_2 and show no or weak response to the presence of glucose. H_2O_2 release follows classical catabolite repression in strains of group III. S. paras., *S. parasanguinis*.

dental microbial community. The metabolic output of SpxB has an intrinsic function for the individual cell by providing energy via acetyl-phosphate production. In addition, the excretion of H_2O_2 provides an ecological advantage for the H_2O_2-tolerant community by increasing the concentration of this reactive oxygen species in the immediate vicinity of the producer. This has the potential to negatively affect or outcompete H_2O_2-susceptible species and favors the integration of H_2O_2-compatible species into the biofilm. Therefore, SpxB seems to play an important ecological role in dental biofilm formation (24).

The wide distribution of *spxB* as an oral streptococcal community-expressed gene with metabolic and ecological impact makes it important to understand that *spxB* expression might be differentially controlled by regulatory proteins or *cis*-regulatory promoter regions. As presented here, seemingly conserved regulatory elements present in *S. sanguinis* and *S. gordonii* regulate *spxB* expression differently. The unexpected regulatory role of CcpA in *S. sanguinis spxB* expression might even extend to several other genes, since expression of *eno*, *ldh*, *ccpA*, *pykF*, and *manL*, all having predicted *cre* binding sites, is also not influenced by different glucose concentrations (Fig. 9). Furthermore, some of these genes are downregulated after deletion of *ccpA* (Fig. 10), indicating a positive regulatory effect by CcpA. One gene is even regulated in an opposing way (*manL*) in both species. CcpA is the central carbon catabolite regulator in Gram-positive bacteria and regulates the major response of the bacterial cell to the availability and quality of carbohydrates (34). CcpA interacts with HPr (histidine phosphocarrier protein), which is phosphorylated at specific serine 46 (Hpr-Ser46-p) in response to high concentrations of glycolytic intermediates that are present during growth with the favored carbohydrate glucose (39, 45, 46). The interaction of both proteins results in the binding of CcpA to the promoter regions of genes subjected to carbon catabolite control (33). An important functional element for the regulatory role of CcpA is its *cre* binding site located in the promoter region of respective genes (33, 47). Binding of CcpA to the highly degenerate, pseudopalindromic *cre* sequence usually results in repression of CCR-sensitive operons (48). In addition to CCR, carbon catabolite

activation (CCA) also has been described (49). This activating effect of CcpA is an additional regulatory mechanism that provides competitive advantages during carbon catabolism (50).

Our initial investigation using the RegPrecise database (37), a collection of manually curated regulons in prokaryotic genomes, showed the presence of two binding sites in the *S. gordonii* $spxB_p$ but only one in the *S. sanguinis* $spxB_p$. The consensus sequence for *cre* in streptococcaceae was determined based on 968 individual *cre* sites and consists of 16 nucleotides. Positions 5 (A), 6 (A), 8 (C), 9 (G), 11 (T), and 12 (T) are strongly conserved (Fig. 3C). The overall conserved region at nucleotide positions 8 and 9 might explain why no second *cre* site was predicted in *S. sanguinis* despite an overall conservation of the promoter sequence between *S. gordonii* and *S. sanguinis*. T (position 8) and A (position 9) replace both positions in *S. sanguinis*. DNA footprint analysis and mutational studies confirmed binding of CcpA to both *cre* 1 and *cre* 2 in the *S. sanguinis spxB* promoter using the described experimental *in vitro* conditions. Binding to *cre* 2 might be weaker due to less conservation of the binding site. In addition, binding of CcpA might be fine-tuned under *in vivo* conditions, since other effectors, like HPr, determine binding affinities. Furthermore, the presence of high- and low-affinity *cre* sites in the genome might direct CcpA at higher concentrations to less conserved binding sites, as demonstrated for *Bacillus subtilis* (51). Therefore, the presence of a weaker, less conserved *cre* site might have biological relevance under certain growth conditions.

The observed *spxB* expression difference between *S. sanguinis* and *S. gordonii* in the presence of increased glucose concentrations is not explainable by the *cre* sites in the promoter sequence alone, which is supported by our promoter swap experiments that did not alter cell-specific regulation. Similarly, exchanging the CcpA protein itself did not transfer the regulation specific for one species to the other. We therefore compared the structure predictions of CcpA between *S. sanguinis* and *S. gordonii*, which were modeled on the solved structure of CcpA from *B. subtilis*. The DNA binding motif is 100% conserved between both species, and both proteins were able to bind the *spxB* promoter of the other species. This is also reflected in the similar HTH architecture in the model predictions. However, the structural modeling showed an α-helical region in *S. gordonii*, which seems to be replaced by a loop in *S. sanguinis*. Since this loop is not located in the interaction domain with HPr, it is intriguing to speculate that other effector proteins or components interact at this position and that the overall species-specific regulation is upstream of CcpA. This is further supported by the observation that the distinct regulatory patterns are not transferable between SK36 and DL1 by promoter or CcpA exchange. One possible effector could be an alternative HPr differently affecting CcpA-dependent catabolite repression, similar to CrH in *Bacillus subtilis* (41). However, amino acid-based BLAST searches in the SK36 and DL1 genomes did not identify an alternative HPr present in either species. Nevertheless, a possible effector influencing CcpA activity, which is different from an alternative HPr, cannot be ruled out and seems to be a reasonable explanation for the regulative discrepancy found here between the investigates species.

It is also possible that *S. sanguinis* shifted to a more pronounced CcpA interaction with other effector molecules. For example, a glucose-independent, CcpA-dependent regulation has been shown for several genes in different species, including *B. subtilis*, *Staphylococcus aureus*, and *Clostridium difficile* (52–54). It has also been reported that CcpA can respond to NAD, and it is therefore possible that CcpA controls *spxB* expression based on the oxidoreduction potential of the cell (55).

Alternatively, posttranslational regulation mechanisms by small RNAs might play a role in the observed differential regulation here. Small noncoding RNAs regulate diverse cellular processes and are not necessarily present or active in all members of the same species (56–58). However, due to the fact that the differences in SK36 and DL1 also were present in the luciferase reporter assay, posttranslational regulation might play a minor role in explaining the divergent H_2O_2 phenotypes of SK36 and DL1.

Biologically, this adaptation might be explained by the need to tightly control H_2O_2

production under aerobic growth conditions, since *S. sanguinis* is more susceptible to its own H_2O_2 production than *S. gordonii* (59). Furthermore, a differential response to other molecules, like glucose 6-phosphate and fructose 1,6-bisphosphate, is possible, although this requires the presence of HPr-Ser46-p (60).

In addition to the differences within the *cre* sequences, which possibly influence the CcpA-dependent repression of *spxB* transcription, SK36 has a reduced distance between the ribosomal binding site (RBS; or Shine-Dalgarno [SD] sequence) and the ATG start codon of *spxB* compared to the sequence of DL1. In SK36 the distance is 7 nucleotides, whereas in DL1 the distance is 10 nucleotides, which is the distance in the majority of the surveyed streptococcal sequences (http://www.ncbi.nlm.nih.gov). In detail, of 77 available *spxB* promoter sequences, 68 possess a 10-nucleotide distance between the RBS (5′-AGGAG-3′) (42) and the *spxB* start codon: *S. pneumoniae*, 47 sequences available; *S. gordonii*, 5; *S. oralis*, 4; *S. mitis*, 3; *S. pseudopneumoniae*, 1; *S. cristatus*, 1; *S. anginosus*, 1; *Streptococcus* spp., 6. The remaining sequences show an RBS-ATG distance of 7 nucleotides (*S. parasanguinis*, 2; *S. sanguinis*, 1; *S. salivarius*, 1; *S. himalayensis*, 1; *Streptococcus* spp., 2). These different spacer lengths could dramatically influence the expression efficiency of the respective gene (61). Besides an altered translation initiation frequency, a suboptimal RBS-ATG distance could cause reduced mRNA stability or elevated premature transcription termination leading to hampered expression (62).

However, the distance did not influence *spxB* expression, since the *spxB* expression profile could not be transferred via promoter exchanges (which included the respective RBS-ATG spacer). No significant differences could be observed between the native and the heterologous promoter in SK36 and DL1, either in H_2O_2 release (Fig. 6 and 7) or in the luciferase reporter activity assay (Fig. 8). This suggests that the differences in *spxB* expression are not caused by the different SD-ATG spacer lengths in these two strains. This conclusion is further underlined by the differentially regulated H_2O_2 release of the investigated clinical isolates and their respective promoter sequences. The SD-ATG spacer lengths are very heterogenic across species and across the three groups differing in their H_2O_2 phenotype postulated here. These findings further support the idea of a CcpA-dependent but carbohydrate-independent regulation of *spxB* in *S. sanguinis*. Further investigations are under way.

Interestingly, we discovered that other SpxB-positive streptococci that form the oral cavity fall into one of three categories: I, high-level H_2O_2 production, CCR insensitive; II, low-level H_2O_2 production, CCR insensitive; and III, CCR-sensitive decreased H_2O_2 production. Surprisingly, sequencing of the respective promoter regions uncovered a very heterogenic organization of *cre* boxes and different SD-ATG spacer lengths within these groups and even within species (see Fig. S4 in the supplemental material).

Whether this scheme of categorization is broadly distributed among oral streptococci needs to be verified. Intriguingly, this observation fully supports the need to understand the genetic regulation of pathways important in oral bacteria. Overall, this study shows that conservation of a metabolic pathway, including respective regulatory mechanisms, does not correspond to similar regulation and expression. Global approaches to understanding oral microbial ecology and its association with disease development, including metatranscriptomics, are not able to unravel such differences easily. However, at this point it is not known if the functional SpxB output is associated with disease or oral health. A limited number of studies have been performed so far. Notably, the expression of *spxB* was modestly increased in *S. gordonii*, *S. sanguinis*, and *S. oralis* in two out of three patients with generalized aggressive periodontitis (44). Conclusions drawn from this study are limited due to the low number of subjects analyzed. Furthermore, SpxB confers a significant physiological advantage for *S. gordonii*, since an SpxB mutant is less infectious in a murine model of abscess formation (63). Overall the importance of SpxB for oral streptococcal ecology has been shown *in vivo* and *in vitro*. Further experimental evidence is needed to fully appreciate the role in disease and health as well as the significance of the differential regulation in oral biofilm ecology described here.

TABLE 1 Strains and plasmids used in this study

Strain or plasmid	Relevant characteristic(s)	Reference or source
S. gordonii DL1	Wild type	64
S. sanguinis SK36	Wild type	ATCC BAA-1455
S. mitis 12261	Wild type	65
S. oralis J22	Wild type	66
S. parasanguinis	Wild type, clinical isolate	25
S. infantis	Wild type, clinical isolate	25
S. gordonii DL1 Δ*ccpA*	*ccpA* deletion mutant (*ccpA*::*ermAM*)	31
S. sanguinis SK36 Δ*ccpA*	*ccpA* deletion mutant (*ccpA*::*ermAM*)	35
S. gordonii DL1 Δ*spxB*	*spxB* deletion mutant (*spxB*::*ermAM*)	67
S. sanguinis SK36 Δ*spxB*	*spxB* deletion mutant (*spxB*::*ermAM*)	67
S. gordonii DL1 *ccpA*::$ccpA_{(SK36)}$	Expression of heterologous CcpA from SK36, Spc^r	This study
S. gordonii DL1 $spxB_{p(SK36)}$-*spxB*	*spxB* expression under the control of hererologous *spxB* promoter of SK36, Spc^r	This study
S. gordonii DL1 $spxB_{p(DL1)}$-*luc*	*spxB* luciferase reporter (natural *spxB* promoter), Spc^r	This study
S. gordonii DL1 $spxB_{p(SK36)}$-*luc*	*spxB* luciferase reporter (heterologous *spxB*-promoter of SK36), Spc^r	This study
S. sanguinis SK36 *ccpA*::$ccpA_{(DL1)}$	Expression of heterologous CcpA from DL1, Spc^r	This study
S. sanguinis SK36 $spxB_{p(DL1)}$-*spxB*	*spxB* expression under the control of heterologous *spxB*-promoter of DL1, Spc^r	This study
S. sanguinis SK36 $spxB_{p(SK36)}$-*luc*	*spxB* luciferase reporter (natural *spxB*-promoter), Spc^r	This study
S. sanguinis SK36 $spxB_{p(DL1)}$-*luc*	*spxB* luciferase reporter (heterologous *spxB*-promoter of DL1), Spc^r	This study
E. cloni 10G	*E. coli* cloning strain, Amp^r	Lucigen, WI
E. coli BL21(DE3) pLysS	Protein expression strain, Cpm^r	Promega, WI
BL21(DE3) pLysS(pET29b(+) + *Sg CcpA*)	Expression of CcpA of DL1, Kan^r Cpm^r	This study
BL21(DE3) pLysS(pET29b(+) + *Ss CcpA*)	Expression of CcpA of SK36, Kan^r Cpm^r	This study
pDL 278	*E. coli-Streptococcus* shuttle vector, Spc^r	68
pET 29b(+)	N-terminal 6× His fusion protein expression vector; Kan^r	Novagen/Milliore Sigma, MA
pFW5-luc	Suicide vector; Spc^r	69

MATERIALS AND METHODS

Bacterial strains, plasmids, and media. The plasmids and bacterial strains used in this study are listed in Table 1. *Streptococcus* strains were grown in liquid or on agar-solidified BBL brain heart infusion (BHI; Becton Dickinson & Co., Sparks, MD) under aerobic conditions (5% CO_2). *Escherichia coli* strains were grown in Difco lysogeny broth (LB; Lennox, Becton Dickinson & Co., Sparks, MD) or on agar-solidified LB at 37°C. Glucose was added to the medium when indicated from a filter-sterilized 20% stock solution. The following antibiotics were supplemented for selection: kanamycin (100 μg ml^{-1}), erythromycin (10 μg ml^{-1}), and spectinomycin (200 μg ml^{-1}).

DNA manipulations. Standard nucleic acid recombinant protocols were used (70). Restriction enzymes were procured from New England BioLabs (Beverly, MA). DNA ligase, pGEM-T, and GoTaq-DNA polymerase were purchased from Promega (Madison, WI). All plasmids were extracted using the PureYield plasmid miniprep system kit or the Wizard plus SV minipreps DNA purification system (Promega). Accuprime Pfx DNA polymerase was obtained from Life Technologies. PCR products were purified using a Qiagen QIAquick PCR purification kit (Valencia, CA) or Wizard SV gel and PCR clean-up system (Promega). Oligonucleotides were synthesized by Integrated DNA Technologies (IDT; Coralville, IA).

Exchange of *ccpA*. To determine if the different CcpA-dependent repression patterns of *spxB* in SK36 and DL1 are caused by differences in the *ccpA* gene sequence itself, the *ccpA* gene was exchanged between SK36 and DL1. Therefore, upstream and downstream fragments of *ccpA*, *ccpA* itself, and the *aad9* spectinomycin resistance cassette were amplified by PCR utilizing Platinum Pfx DNA polymerase (Invitrogen). Subsequently, the four fragments were fused together in an overlapping PCR. The resulting amplicons were transformed into DL1 Δ*ccpA* and SK36 Δ*ccpA* strains, generating the *S. gordonii* DL1 Δ*ccpA*::$ccpA_{(SK36)}$ and *S. sanguinis* SK36 Δ*ccpA*::$ccpA_{(DL1)}$ strains with the following chromosomal arrangement: upstream gene-exchanged *ccpA-aad9*-downstream gene.

In detail, the primer pairs CP1_SG_US_F/CP1_SG_US_R (DL1) and SS_DS_F_N/SS_up_R_OL (SK36) were utilized to amplify the upstream fragments. The *ccpA* genes were amplified with the primer pairs CP2_SG_SKP1_F/SR_ccpA_Ss_R_spec (SK36) and HR_ss_dl1_F/SR_ccpA Sg_R_spec (DL1). The *aad9* gene from pDL278 was amplified with the primer pairs SR_aad9_F_CP12/SR_aad9_R_Sg [for *S. gordonii* DL1 Δ*ccpA*::$ccpA_{(SK36)}$] and SR_aad9_F/SR aad9_R_Ss [for *S. sanguinis* SK36 Δ*ccpA*::$ccpA_{(DL1)}$]. The downstream fragments were generated with the primer pairs SR_ccpA_Sg_ds_F/CP1_SG_DS_R (DL1) and SR_ccpA_Ss ds_F/DS_ss_R (SK36). The primers introduced overlapping sequences between the PCR fragments, allowing the PCR-based fusion of all three fragments.

For overlapping PCR, 0.5 μl of the unpurified PCR products was added directly to 22.5 μl Platinum Pfx DNA polymerase reaction mixture by following the manufacturer's manual. After 10 initial cycles with 80 s of elongation time, the primer pairs CP1_SG_US_F/CP1_SG_DS_R [DL1 Δ*ccpA*::$ccpA_{(SK36)}$] and SS_DS_F_N/DS_ss_R [SK36 Δ*ccpA*::$ccpA_{(DL1)}$] were added, followed by 30 additional amplification cycles (225 s of elongation). The resulting amplicon was transformed into naturally competent DL1 Δ*ccpA* and

SK36 Δ*ccpA* strains by adding competence-stimulating peptide (CSP). Correct introduction of *ccpA* was verified by PCR and sequencing.

Promoter exchange of *spxB*. To test if the differences in the *spxB* expression of SK36 and DL1 are caused by differences in promoter sequences, the respective promoters were exchanged between the two strains. Therefore, a fragment upstream of the *spxB* promoter, *aad9*, the promoter sequence, and a part of *spxB* were amplified and introduced into an overlapping PCR as described above. Subsequently the resulting amplicons were transformed into wild-type DL1 and SK36 to generate *S. gordonii* DL1 $spxB_{P(SK36)}$-*spxB* and *S. sanguinis* SK36 $spxB_{P(DL1)}$-*spxB* strains. The resulting chromosomal arrangement is upstream gene-*aad9*-exchanged *spxB*-promoter-*spxB*. Correct promoter replacement was verified by PCR and sequencing.

In detail, the upstream fragments were amplified with the primer pairs Ss_spxB_Pex_UF/Ss_spxB-_Pex_UR (SK36) and Sg_spxB_Pex_UF/Sg_spxB_Pex UR (DL1). *aad9* was amplified with the primers SR_aad9 F_CP12 and SR_aad9_R_Ss using pDL278 as the template. Promoter sequences were amplified with the primer pairs Sg_spxB_Pex_PF/Sg_spxB_Pex_PR_2 (DL1) and Ss_spxB_Pex_PF/Ss_spxB_Pex_PR (SK36). The downstream fragments were amplified with the primer pairs Ss_spxB_Pex_DF_2/Ss_spxB-_Pex_DR (SK36) and Sg_spxB_Pex_DF/Sg_spxB_Pex_DR. The primer pairs Ss_spxB_Pex_UF/Ss_spxB-_Pex_DR and Sg_spxB_Pex_UF/Sg_spxB_Pex_DR were used for overlapping PCR as described above.

Construction of $spxB_p$-luciferase reporter strains. To verify the already-described differentially regulated expression of *spxB* and to confirm the results of *spxB* expression after *spxB*-promoter exchange on the transcription level, four $spxB_p$-luciferase reporter strains were constructed: *S. sanguinis* SK36 $spxB_{P(SK36)}$-*luc* and *S. gordonii* DL1 $spxB_{P(SK36)}$-*luc* strains, with the firefly luciferase gene (*luc*) under the control of the *spxB* promoter of SK36, as well as *S. sanguinis* SK36 $spxB_{p(DL1)}$-*luc* and *S. gordonii* DL1 $spxB_{p(DL1)}$-*luc* strains, with *luc* under the control of the *spxB* promoter of DL1. Therefore, suicide plasmids were constructed containing an ~600-bp sequence with the *spxB* promoter controlling the firefly luciferase gene *luc*. Additionally, an ~1-kb sequence of the 5′ region of *spxB* was introduced for the chromosomal integration of the plasmid. The resulting plasmids were transformed into *S. sanguinis* SK36 and *S. gordonii* DL1.

The 5′ *spxB* fragment (for integration) was fused in the inverted direction to the 3′ end of the *spxB* promoter fragment via fusion PCR. Thus, in the final reporter strains, one copy of *spxB* remained unaffected under the control of its natural promoter. Additionally, the expression of the $spxB_p$-controlled *luc* was not affected by the transcription of upstream genes. The final chromosomal arrangement in all generated strains was upstream region of *spxB*-*spxB*-integrated vector-*luc* (complement [comp.])-*spxB* promoter (comp.)-truncated 5′ region of *spxB*-downstream sequence of *spxB*. Correct integration was verified by PCR and sequencing.

In detail, the *spxB* promoter region was amplified from SK36 and DL1 using the primer pairs Ss_spxB_luc_PF/SG_spxB_luc_PR and Sg_spxB_luc_PF/SG_spxB_luc_PR, respectively. The ~1,000-bp fragment spanning the 5′ region of *spxB* and the partial downstream gene was amplified using the primer pairs SG_spxB_luc_IR/Sg_spxB_luc_IF and SG_spxB_luc_IR/Ss_spxB_luc_IF. The 5′ *spxB* sequence amplified from SK36 and DL1 was fused to the *spxB* promoter of the same species (luciferase assay of the natural *spxB* promoter) or to the *spxB* promoter of the other species (luciferase assay of the *spxB* promoter exchange), respectively. The overlapping PCR was performed as described above with the primer pair SG_spxB_luc_IR/SG_spxB_luc_PR. The resulting fragment was purified, BglII/SalI digested, and cloned into BamHI/SalI-digested *pFW5-luc*. Correct integration was verified by PCR and sequencing. Transformation into SK36 and DL1 was performed as described above.

Luciferase assay. Luciferase assays using $spxB_p$-luciferase reporter strains of *S. gordonii* DL1 and *S. sanguinis* SK36 were carried out as described earlier (35, 71). Briefly, cells from an overnight culture were harvested, washed with phosphate-buffered saline (PBS), and adjusted to an optical density at 600 nm (OD_{600}) of 0.5. Subsequently, 4 ml BHI medium (with and without the addition of 2% glucose) was inoculated to a final OD_{600} of 0.05. The cultures were incubated at 37°C under aerobic conditions (200 rpm) for 5 h.

The luciferase activity was measured using a GloMax Discover (Promega). Therefore, 200 μl of cell culture was mixed with 50 μl of 1 mM D-luciferin (suspended in 100 mM citrate buffer, pH 6; Sigma). Specific luciferase activity is presented as relative light units (RLU) normalized to the absorption of the bacterial culture at 600 nm. Presented are averages and standard deviations from five independent experiments performed with three technical replicates each.

Measurement of relative H_2O_2 production. H_2O_2 indicator plates were prepared as described previously (36). Overnight cultures of *S. gordonii* DL1 and *S. sanguinis* SK36 strains were washed in PBS and adjusted to an OD_{600} of 0.5. Indicator plates supplemented with and without 2% glucose were inoculated with 12 μl of PBS-washed cells and incubated overnight in the presence of 5% CO_2. H_2O_2 generation was determined by measuring the distance between the edge of the colony and the end of the precipitation zone (Fig. 1C). All experiments were performed with two technical replicates and at least three independent experiments.

qRT-PCR. Quantitative real-time PCR (qRT-PCR) was performed for a subset of genes of *S. sanguinis* SK36 and *S. gordonii* DL1. CcpA-regulated genes with at least one *cre* site in the promoter region were selected on the basis of the public database RegPrecise (37). Primers generating PCR amplicons of 210 to 280 bp were designed with the help of the free public online tool PrimerFox (http://www.primerfox.com) and are shown in Table 2.

Total RNA was isolated as follows. *S. gordonii* DL1 as well as *S. sanguinis* SK36 cells (wild types and *ccpA* deletion mutants) were grown overnight, harvested, and washed with PBS. Fresh BHI medium (with and without the addition of 2% glucose) was inoculated to a final OD_{600} of 0.05 with PBS-washed cells.

TABLE 2 Oligonucleotides used in this study[a]

Primer name	Sequence (5′–3′)
CP1_SG_US_F	CAA ACC GTG GTA TTT AGT TAA AAT TAA
CP1_SG_US_R	GTC TGT GTT CAT ATT GCT TCC TTT CTT AAA GTT GAA AAT AA
SS_DS_F_N	TTG GTC AAA ATC AAG TTG TCA AAC
SS_up_R_OL	GTC TGT GTT CAT ATA GTT TCC TTT C
CP2_SG_SKP1_F	GAA AGG AAG CAA TAT GAA CAC AGA CGA CAC AGT AAC
SR_ccpA_Ss_R_spec	CAT GTA TTC ACG AAC GAA AAT CGA TCT TAT TTC CGA GTT GAT TTA CGC TC
HR_ss_dl1_F	GAA AGG AAA CTA TAT GAA CAC AGA CGA TAC AGT AAC
SR_ccpA_Sg_R_spec	CAT GTA TCA CGA ACG AAA ATC GAT CTT ATT TTC TAG TTG AGT TCC GTT CG
SR_aad9_F_CP12	GAT CGA TTT TCG TTC GTG AAT ACA TG
SR_aad9_R_Sg	CTC TTC CAT GGA CGA GAA AGT TAT GCA AGG
SR aad9_R_Ss	GCA TGC ATG GAC GAG AAA GTT ATG CAA GG
SR_ccpA_Sg_ds_F	GCA TAA CTT TCT CGT CCA TGG AAG AGT TGG AAG AAC GTG
CP1_SG_DS_R	AAG CTT TTT AGA ATA CTC TGA CGG
SR_ccpA_Ss_ds_F	GCA TAA CTT TCT CGT CCA TGC ATG CTG ACT AAG ATT ATG C
DS_ss_R	CCT TGG TCG AAT GCC CAT G
Ss_spxB_Pex_UF	CCT GAT AGG TAC CAA TGA C
Ss_spxB_Pex_UR	CAT GTA TTC ACG AAC GAA AAT CGA TCT ACA TAA CAC CAA GCC CTG
Sg_spxB_Pex_UF	GGA TAT TGC GAT CGA GTC C
Sg_spxB_Pex UR	CAT GTA TTC ACG AAC GAA AAT CGA TCC TAT TAC ATA ACA GAT GCT C
Sg_spxB_Pex_PF	GCA TAA CTT TCT CGT CCA TGC ATG CGG ATT CCA ATT GCT GCT GG
Sg_spxB_Pex_PR_2	GCA GTA ATT TTT CCT TGA GTC ATA AGA ATA ACT CTC CTT C
Ss_spxB_Pex_PF	GCA TAA CTT TCT CGT CCA TGC ATG CAG ATC CAA TTG CTG TCG
Ss_spxB_Pex_PR	GCA GTA ATT TTC CCT TGA GTC ATA ATA ACT CTC CTT C
Ss_spxB_Pex_DF_2	GAG TTA TTC TTA TGA CTC AAG GAA AAA TTA CTG C
Ss_spxB_Pex_DR	CGC TCA TAA GAA CCT GAT CC
Sg_spxB_Pex_DF	GAG TTA TTA TGA CTC AAG GGA AAA TTA CTG C
Sg_spxB_Pex_DR	CGT TCG TAT GAA CCT GAA CC
Ss_spxB_luc_PF	CCTACGTCGATTGACGCAGATCCAATTGCTGTCG
SG_spxB_luc_PR	ATTA AGA TCT GAG CAT TGC TGC AGA TGC AG
Sg_spxB_luc_PF	CCT ACG TCG ATT GAT GGG ATT CCA ATT GCT GCT G
SG_spxB_luc_IR	ATTA GTC GAC AGG CAR TGA ATG CCA ATC G
Sg_spxB_luc_IF	GCA ATT GGA ATC CCA TCA ATC GAC GTA GGT GAC AC
Ss_spxB_luc_IF	GCA ATT GGA TCT GCG TCA ATC GAC GTA GGT GAC AC
Sg CcpA F	ATTA CAT ATG AAC ACA GAC GAT ACA G
Sg CcpA R	ATTTA CTC GAG TTT TCT AGT TGA GTT CCG
Ss CcpA F	ATTA CAT ATG ACA GAC GAC ACA GTA ACG
Ss CcpA R	ATTTA CTC GAG CCG AGT TGA TTT ACG CTC G
Sg EMSA spxB RP	5Biosg/TGC AGA TGC AGT AAT TTT TCC CTT GA
Sg EMSA spxB FP	CAG CTA CAA GTC TTA GAG GTG CAT
Sg spxB RP	TGC AGA TGC AGT AAT TTT TCC CTT GA
ss rp spxB emsa	5Biosg/TGC AGA TGC AGT AAT TTT TCC TTG
ss fp spxB emsa	CAG GGC TTG GTG TTA TGT AAT AG
ss rp spxB	TGC AGA TGC AGT AAT TTT TCC TTG
Ss NiaX FP	CAA GTC CAG CAG AAC ACT A
Ss NiaX RP Bio	5Biosg/GGT TTC ATA GTG ACT CCT TTT
Ss NiaX RP	GGT TTC ATA GTG ACT CCT TTT
spxB FAM F	FAM-GTA ATA GTT CTA TAT CAT CTT TGA GC
spxB VIC R	VIC-CAT AAT AAC TCT CCT TCA ATA AAA TAA ATT
Sot_Si_spxB_seq_UF	CAA GCC YTG CAY GGR AAA GGT G
Sot_Si_spxB_seq_UR	CAA GAG CAC CTG TTT CTT CG
spxB G checker F	TTG TAG GAC TGG GAT TGA CC
spxB_RNA_check_UR	ACC GTT AAT CAA GTG AGT CG
Scr_spxB_seq_UFa	CTT GCT TTA GTC TAR CCA YTG G

[a]Recognition sequences for restriction enzymes BglII, SalI, NdeI, and XhoI are underlined.

The cultures were incubated at 37°C under aerobic conditions (200 rpm) for 5 h. Subsequently, cells were harvested (11,000 × *g* for 15 min at 4°C). Cell pellets were stored at −80°C until further use. Total RNA extraction was done by following the TRIzol method according to the manufacturer's manual, including mechanical disruption of cells with the Precellys evolution homogenizer (Bertin Technologies, Rockville, MD) (4 rounds of 30 s each at 8,300 rpm, with incubation on ice). After being DNase I treated (Invitrogen) for 2 h, total RNA was cleaned with the Qiagen RNeasy kit by following the manufacturer's protocol. Subsequently, cDNA was synthesized from 2 μg of RNA using SuperScript II reverse transcriptase (Invitrogen), and qRT-PCR was performed on a CFX connect real-time PCR detection system (Bio-Rad) using SYBR green master mix (Bio-Rad) according to the manufacturer's instructions. qRT-PCR conditions were 7 min at 95°C, 15 s at 95°C, 30 s at 56°C, and 30 s at 72°C. The last three steps were repeated 40 times. Each assay was performed with three biologically independent RNA samples in technical duplicates.

Threshold cycle (C_T) values were determined and data were analyzed with Bio-Rad CFX Manager software (version 2.0). Relative quantification was performed with the comparative C_T method ($2^{-\Delta\Delta CT}$). The 16S rRNA gene was used as the housekeeping reference control.

Overexpression and purification of CcpA. Using oligonucleotides Sg CcpA F/R, Ss CcpA F/R PCR amplification was carried out using DL1 or SK36 chromosomal DNA as the template. The amplified *ccpA* fragments were digested with NdeI/XhoI restriction enzymes and ligated into pET-29b(+). The ligated vector was transformed into *E. cloni* 10G competent cells (Lucigen, Middleton, WI). For overexpression, isolated and confirmed plasmids were transformed into *E. coli* BL21(DE3) pLysS. Overexpression was achieved with the addition of 1 mM isopropyl-β-D-thiogalactopyranoside (IPTG), incubation for 5 h at 37°C, and agitation at 200 rpm. The overexpressed *S. gordonii* CcpA His-tagged protein was purified under nondenaturing conditions using Ni-nitrilotriacetic acid (Ni-NTA)–agarose matrix (Invitrogen) per the manufacturer's instructions. The *S. sanguinis* CcpA His-tagged protein was purified using a denaturation-renaturation method. Briefly, overexpressed cells were resuspended in lysis buffer (50 mM Tris-HCl, 1 mM EDTA) and sonicated (30-s pulse and 1-min intervals) 10 times and centrifuged at 12,000 rpm for 10 min at 4°C. The obtained pellet was washed with three volumes of wash buffer (10 mM Tris-HCl, 300 mM NaCl, 1 mM EDTA, 1% Triton X-100, and 1 M urea) and thoroughly washed with water five times. Further, the pellet was dissolved in renaturation buffer (50 mM Tris-HCl, 5 mM $MgCl_2$, 2.5 mM β-mercaptoethanol, 0.1% Tween 20, and 8 M urea) and incubated at room temperature for 1 h. The supernatant was dialyzed against decreasing concentrations of urea containing renaturation buffer (6 M to 1 M). The protein concentration was determined using the Pierce bicinchoninic acid protein assay kit with bovine serum albumin (BSA) as the standard. Purified protein was aliquoted, lyophilized, and stored at −80°C for further use.

EMSA. 5′-biotin-labeled oligonucleotides (Sg spxB EMSA R/Ss spxB EMSA R) were synthesized by IDT. Biotin-labeled and unlabeled *spxB* probes were PCR amplified using *S. gordonii* DL1 and *S. sanguinis* SK36 chromosomal DNA. For engineered promoter probes either deleting *cre* sites or introducing *cre* sites into an unrelated promoter, gBlock gene fragments were synthesized by IDT and used as the template for PCR with the respective 5′-biotin-labeled oligonucleotides. Purified CcpA was incubated at various concentrations (20 to 160 pmol) with the biotin-labeled DNA probes (1 fmol) in binding buffer [10 mM Tris-HCl, pH 7.4, 50% glycerol, 1 mM $MgCl_2$, NP-40, and 1 μg/μl poly(dI · dC)] for 1 h at 37°C. After incubation, the reaction mixture was loaded onto 6% acrylamide gels in 0.5× Tris-borate-EDTA (TBE) buffer and separated at 100 V for 1 h. Subsequently, the DNA-protein complex was transferred to a positively charged Hybond-N+ nylon membrane (Amersham) and UV cross-linked in a UV cross-linker for 1 min (Stratagene). The DNA-protein complex was detected using a LightShift chemiluminescent EMSA kit (Thermo Scientific). For the competition assay, various concentrations (ranging from 1 fmol to 500 fmol) of unlabeled $spxB_p$ probe were added to the reaction mixture, and EMSA was carried out as described above.

Generation of *spxB* and *niaX* promoter constructs for EMSA. Promoter fragments of *spxB* and *niaX* containing deleted or introduced *cre* sites were synthesized as gBlocks gene fragments, and sequences were verified by Integrated DNA Technologies (Coralville, IA).

Structural modeling of CcpA. The I-TASSER protein structure and function prediction algorithm (40) was used to model CcpA from *S. gordonii* and *S. sanguinis* with the solved crystal structure of PDB entry 1ZVV (CcpA from *Bacillus subtilis*) as the template. The resulting structural predictions were visualized using UCSF chimera molecular visualization software.

DFACE. DFACE was performed as previously described (72). Briefly, the *spxB* promoter region was amplified from SK36 chromosomal DNA with the fluorescent dye-labeled oligonucleotides spxB FAM F (5′ 6-carboxyfluorescein [FAM]-GTA ATA GTT CTA TAT CAT CTT TGA GC-3′) and spxB VIC R (5′ VIC-CAT AAT AAC TCT CCT TCA ATA AAA TAA ATT-3′). Various concentrations of CcpA (0, 5, 10, and 15 μg) were incubated with binding buffer [10 mM Tris-HCl, pH 7.4, 50% glycerol, 1 mM $MgCl_2$, NP-40, and 2 μg/μl poly(dI · dC)] for 15 min at room temperature. In parallel, control reactions were carried out without protein and with BSA. After incubation, 100 ng of fluorescence-labeled probes was added and incubated at 37°C for 1 h. To the reaction mixture, 0.002 kU of DNase I (Worthington Biochemicals, Lakewood, NJ) was added and incubated at room temperature for 5 min. The digestion reactions were terminated immediately by incubating at 75°C for 10 min. The probes were purified using the MinElute reaction cleanup kit (Qiagen, Valencia, CA) and eluted with nuclease-free water. The fragments were analyzed with the 3730 DNA analyzer (Plant-Microbe Genomics Facility, The Ohio State University). Each probe (0.5 μl) was mixed with 9 μl of Hi-Di formamide and 0.1 μl of Gene Scan-LIZ size standard (Applied Biosystems), injected at 3 kV for 30 s. Obtained electropherograms were analyzed with GeneMapper 4.0 software.

Species identification. Species belonging to the clinical isolates analyzed in this study were determined by sequencing and BLAST comparisons of the 16S RNA gene (https://blast.ncbi.nlm.nih.gov/Blast.cgi). The 16S RNA gene was amplified using universal primers 16s_27f (73) and 16s_1392r (74). In several cases the results were inconclusive due to the close relationship of *S. mitis* and *S. pneumoniae*. To distinguish between these species, a part of the *recA* gene was sequenced and analyzed for species-specific nucleotide polymorphisms as described elsewhere (75).

Sequencing of the *spxB* promoter regions of clinical isolates. The promoter regions have been sequenced using the primer pairs Sot_Si_spxB_seq_UF/Sot_Si_spxB_seq_UR for *S. oralis*, *S. infantis*, and *S. mitis*, spxB_G_checker_F/spxB_RNA_check_UR for *S. parasanguinis*, and Scr_spxB_seq_Ufa/Sot_Si_spxB_seq_UR for *S. dentisani*.

Statistics. A *t* test or paired *t* test was performed to compare two samples under a given condition. The difference was considered statistically significant for a *P* value of <0.05.

Accession number(s). GenBank accession numbers for sequences determined by *spxB* promoter region sequencing are as follows: MG766287 (*Streptococcus oralis* subsp. *tigurinus* J22, *spxB*), MG766288 (*Streptococcus parasanguinis* LZ3, *spxB* promoter), MG766289 (*Streptococcus infantis* LZ2, *spxB*), MG766290 (*Streptococcus parasanguinis* 1-9B, *spxB* promoter), MG766291 (*Streptococcus dentisanii* 2-1B, *spxB* promoter), MG766292 (*Streptococcus mitis* 3-1, *spxB* promoter), MG766293 (*Streptococcus parasanguinis* 1-3B, *spxB* promoter), MG766294 (*Streptococcus parasanguinis* 1-5, *spxB* promoter), MG766295 (*Streptococcus parasanguinis* 1-7, *spxB* promoter), MG766296 (*Streptococcus parasanguinis* 1-10B, *spxB* promoter), MG766297 (*Streptococcus mitis* 2-7, *spxB* promoter), and MG766298 (*Streptococcus mitis* 2-8, *spxB* promoter).

SUPPLEMENTAL MATERIAL

Supplemental material for this article may be found at https://doi.org/10.1128/JB.00619-17.

SUPPLEMENTAL FILE 1, PDF file, 0.9 MB.

ACKNOWLEDGMENTS

We thank Michael R. Zianni (Ohio State University, Columbus) for technical support and advice for the DNase I footprint analysis.

This work was supported by NIH-NIDCR grant DE021726 to J.K. and NIH-NIDCR grants DE021726 and DE022083 to J.M.

We have no conflicts of interest to declare.

REFERENCES

1. Duran-Pinedo AE, Frias-Lopez J. 2015. Beyond microbial community composition: functional activities of the oral microbiome in health and disease. Microbes Infect 17:505–516. https://doi.org/10.1016/j.micinf.2015.03.014.
2. Simon-Soro A, Mira A. 2015. Solving the etiology of dental caries. Trends Microbiol 23:76–82. https://doi.org/10.1016/j.tim.2014.10.010.
3. Struzycka I. 2014. The oral microbiome in dental caries. Pol J Microbiol 63:127–135.
4. Takahashi N, Nyvad B. 2011. The role of bacteria in the caries process: ecological perspectives. J Dent Res 90:294–303. https://doi.org/10.1177/0022034510379602.
5. Wade WG. 2013. The oral microbiome in health and disease. Pharmacol Res 69:137–143. https://doi.org/10.1016/j.phrs.2012.11.006.
6. Zarco MF, Vess TJ, Ginsburg GS. 2012. The oral microbiome in health and disease and the potential impact on personalized dental medicine. Oral Dis 18:109–120. https://doi.org/10.1111/j.1601-0825.2011.01851.x.
7. Hajishengallis G, Lamont RJ. 2012. Beyond the red complex and into more complexity: the polymicrobial synergy and dysbiosis (PSD) model of periodontal disease etiology. Mol Oral Microbiol 27:409–419. https://doi.org/10.1111/j.2041-1014.2012.00663.x.
8. Lamont RJ, Hajishengallis G. 2015. Polymicrobial synergy and dysbiosis in inflammatory disease. Trends Mol Med 21:172–183. https://doi.org/10.1016/j.molmed.2014.11.004.
9. Xu P, Gunsolley J. 2014. Application of metagenomics in understanding oral health and disease. Virulence 5:424–432. https://doi.org/10.4161/viru.28532.
10. Rosan B, Lamont RJ. 2000. Dental plaque formation. Microbes Infect 2:1599–1607. https://doi.org/10.1016/S1286-4579(00)01316-2.
11. Diaz PI, Chalmers NI, Rickard AH, Kong C, Milburn CL, Palmer RJ, Jr, Kolenbrander PE. 2006. Molecular characterization of subject-specific oral microflora during initial colonization of enamel. Appl Environ Microbiol 72:2837–2848. https://doi.org/10.1128/AEM.72.4.2837-2848.2006.
12. Kirst ME, Li EC, Alfant B, Chi YY, Walker C, Magnusson I, Wang GP. 2015. Dysbiosis and alterations in predicted functions of the subgingival microbiome in chronic periodontitis. Appl Environ Microbiol 81:783–793. https://doi.org/10.1128/AEM.02712-14.
13. Simon-Soro A, Guillen-Navarro M, Mira A. 2014. Metatranscriptomics reveals overall active bacterial composition in caries lesions. J Oral Microbiol 6:25443. https://doi.org/10.3402/jom.v6.25443.
14. Becker MR, Paster BJ, Leys EJ, Moeschberger ML, Kenyon SG, Galvin JL, Boches SK, Dewhirst FE, Griffen AL. 2002. Molecular analysis of bacterial species associated with childhood caries. J Clin Microbiol 40:1001–1009. https://doi.org/10.1128/JCM.40.3.1001-1009.2002.
15. Ge Y, Caufield PW, Fisch GS, Li Y. 2008. *Streptococcus mutans* and *Streptococcus sanguinis* colonization correlated with caries experience in children. Caries Res 42:444–448. https://doi.org/10.1159/000159608.
16. Giacaman RA, Torres S, Gomez Y, Munoz-Sandoval C, Kreth J. 2015. Correlation of *Streptococcus mutans* and *Streptococcus sanguinis* colonization and *ex vivo* hydrogen peroxide production in carious lesion-free and high caries adults. Arch Oral Biol 60:154–159. https://doi.org/10.1016/j.archoralbio.2014.09.007.
17. Johnson KP, Hillman JD. 1982. Competitive properties of lactate dehydrogenase mutants of the oral bacterium *Streptococcus mutans* in the rat. Arch Oral Biol 27:513–516. https://doi.org/10.1016/0003-9969(82)90093-0.
18. Kolenbrander PE, Palmer RJ, Jr, Rickard AH, Jakubovics NS, Chalmers NI, Diaz PI. 2006. Bacterial interactions and successions during plaque development. Periodontol 2000 42:47–79. https://doi.org/10.1111/j.1600-0757.2006.00187.x.
19. Kuboniwa M, Tribble GD, James CE, Kilic AO, Tao L, Herzberg MC, Shizukuishi S, Lamont RJ. 2006. *Streptococcus gordonii* utilizes several distinct gene functions to recruit *Porphyromonas gingivalis* into a mixed community. Mol Microbiol 60:121–139. https://doi.org/10.1111/j.1365-2958.2006.05099.x.
20. McNab R, Ford SK, El-Sabaeny A, Barbieri B, Cook GS, Lamont RJ. 2003. LuxS-based signaling in *Streptococcus gordonii*: autoinducer 2 controls carbohydrate metabolism and biofilm formation with *Porphyromonas gingivalis*. J Bacteriol 185:274–284. https://doi.org/10.1128/JB.185.1.274-284.2003.
21. Simionato MR, Tucker CM, Kuboniwa M, Lamont G, Demuth DR, Tribble GD, Lamont RJ. 2006. *Porphyromonas gingivalis* genes involved in community development with *Streptococcus gordonii*. Infect Immun 74:6419–6428. https://doi.org/10.1128/IAI.00639-06.
22. Whitmore SE, Lamont RJ. 2011. The pathogenic persona of community-associated oral streptococci. Mol Microbiol 81:305–314. https://doi.org/10.1111/j.1365-2958.2011.07707.x.
23. Ramsey MM, Whiteley M. 2009. Polymicrobial interactions stimulate resistance to host innate immunity through metabolite perception. Proc Natl Acad Sci U S A 106:1578–1583. https://doi.org/10.1073/pnas.0809533106.
24. Zhu L, Kreth J. 2012. The role of hydrogen peroxide in environmental adaptation of oral microbial communities. Oxid Med Cell Longev 2012:717843. https://doi.org/10.1155/2012/717843.
25. Zhu L, Xu Y, Ferretti JJ, Kreth J. 2014. Probing oral microbial functionality-expression of *spxB* in plaque samples. PLoS One 9:e86685. https://doi.org/10.1371/journal.pone.0086685.
26. Kreth J, Merritt J, Shi W, Qi F. 2005. Competition and coexistence between *Streptococcus mutans* and *Streptococcus sanguinis* in the dental

biofilm. J Bacteriol 187:7193–7203. https://doi.org/10.1128/JB.187.21.7193-7203.2005.
27. Kreth J, Zhang Y, Herzberg MC. 2008. Streptococcal antagonism in oral biofilms: *Streptococcus sanguinis* and *Streptococcus gordonii* interference with *Streptococcus mutans*. J Bacteriol 190:4632–4640. https://doi.org/10.1128/JB.00276-08.
28. Jakubovics NS, Gill SR, Vickerman MM, Kolenbrander PE. 2008. Role of hydrogen peroxide in competition and cooperation between *Streptococcus gordonii* and *Actinomyces naeslundii*. FEMS Microbiol Ecol 66:637–644. https://doi.org/10.1111/j.1574-6941.2008.00585.x.
29. Jagathrakshakan SN, Sethumadhava RJ, Mehta DT, Ramanathan A. 2015. 16S rRNA gene-based metagenomic analysis identifies a novel bacterial co-prevalence pattern in dental caries. Eur J Dent 9:127–132. https://doi.org/10.4103/1305-7456.149661.
30. Torlakovic L, Klepac-Ceraj V, Ogaard B, Cotton SL, Paster BJ, Olsen I. 14 March 2012. Microbial community succession on developing lesions on human enamel. J Oral Microbiol https://doi.org/10.3402/jom.v4i0.16125.
31. Zheng L, Itzek A, Chen Z, Kreth J. 2011. Environmental influences on competitive hydrogen peroxide production in *Streptococcus gordonii*. Appl Environ Microbiol 77:4318–4328. https://doi.org/10.1128/AEM.00309-11.
32. Zheng LY, Itzek A, Chen ZY, Kreth J. 2011. Oxygen dependent pyruvate oxidase expression and production in *Streptococcus sanguinis*. Int J Oral Sci 3:82–89. https://doi.org/10.4248/IJOS11030.
33. Deutscher J. 2008. The mechanisms of carbon catabolite repression in bacteria. Curr Opin Microbiol 11:87–93. https://doi.org/10.1016/j.mib.2008.02.007.
34. Warner JB, Lolkema JS. 2003. CcpA-dependent carbon catabolite repression in bacteria. Microbiol Mol Biol Rev 67:475–490. https://doi.org/10.1128/MMBR.67.4.475-490.2003.
35. Zheng L, Chen Z, Itzek A, Ashby M, Kreth J. 2011. Catabolite control protein A controls hydrogen peroxide production and cell death in *Streptococcus sanguinis*. J Bacteriol 193:516–526. https://doi.org/10.1128/JB.01131-10.
36. Saito M, Seki M, Iida K, Nakayama H, Yoshida S. 2007. A novel agar medium to detect hydrogen peroxide-producing bacteria based on the Prussian blue-forming reaction. Microbiol Immunol 51:889–892. https://doi.org/10.1111/j.1348-0421.2007.tb03971.x.
37. Novichkov PS, Kazakov AE, Ravcheev DA, Leyn SA, Kovaleva GY, Sutormin RA, Kazanov MD, Riehl W, Arkin AP, Dubchak I, Rodionov DA. 2013. RegPrecise 3.0–a resource for genome-scale exploration of transcriptional regulation in bacteria. BMC Genomics 14:745. https://doi.org/10.1186/1471-2164-14-745.
38. Loll B, Saenger W, Biesiadka J. 2007. Structure of full-length transcription regulator CcpA in the apo form. Biochim Biophys Acta 1774:732–736. https://doi.org/10.1016/j.bbapap.2007.03.020.
39. Schumacher MA, Allen GS, Diel M, Seidel G, Hillen W, Brennan RG. 2004. Structural basis for allosteric control of the transcription regulator CcpA by the phosphoprotein HPr-Ser46-P. Cell 118:731–741. https://doi.org/10.1016/j.cell.2004.08.027.
40. Yang J, Yan R, Roy A, Xu D, Poisson J, Zhang Y. 2015. The I-TASSER suite: protein structure and function prediction. Nat Methods 12:7–8. https://doi.org/10.1038/nmeth.3213.
41. Schumacher MA, Seidel G, Hillen W, Brennan RG. 2006. Phosphoprotein Crh-Ser46-P displays altered binding to CcpA to effect carbon catabolite regulation. J Biol Chem 281:6793–6800. https://doi.org/10.1074/jbc.M509977200.
42. Omotajo D, Tate T, Cho H, Choudhary M. 2015. Distribution and diversity of ribosome binding sites in prokaryotic genomes. BMC Genomics 16:604. https://doi.org/10.1186/s12864-015-1808-6.
43. Willenborg J, de Greeff A, Jarek M, Valentin-Weigand P, Goethe R. 2014. The CcpA regulon of *Streptococcus suis* reveals novel insights into the regulation of the streptococcal central carbon metabolism by binding of CcpA to two distinct binding motifs. Mol Microbiol 92:61–83. https://doi.org/10.1111/mmi.12537.
44. Jorth P, Turner KH, Gumus P, Nizam N, Buduneli N, Whiteley M. 2014. Metatranscriptomics of the human oral microbiome during health and disease. mBio 5:e01012-14. https://doi.org/10.1128/mBio.01012-14.
45. Deutscher J, Saier MH, Jr. 1983. ATP-dependent protein kinase-catalyzed phosphorylation of a seryl residue in HPr, a phosphate carrier protein of the phosphotransferase system in *Streptococcus pyogenes*. Proc Natl Acad Sci U S A 80:6790–6794. https://doi.org/10.1073/pnas.80.22.6790.
46. Poncet S, Mijakovic I, Nessler S, Gueguen-Chaignon V, Chaptal V, Galinier A, Boel G, Maze A, Deutscher J. 2004. HPr kinase/phosphorylase, a Walker motif A-containing bifunctional sensor enzyme controlling catabolite repression in Gram-positive bacteria. Biochim Biophys Acta 1697:123–135. https://doi.org/10.1016/j.bbapap.2003.11.018.
47. Hueck CJ, Hillen W, Saier MH, Jr. 1994. Analysis of a cis-active sequence mediating catabolite repression in Gram-positive bacteria. Res Microbiol 145:503–518. https://doi.org/10.1016/0923-2508(94)90028-0.
48. Weickert MJ, Chambliss GH. 1990. Site-directed mutagenesis of a catabolite repression operator sequence in *Bacillus subtilis*. Proc Natl Acad Sci U S A 87:6238–6242. https://doi.org/10.1073/pnas.87.16.6238.
49. Lorca GL, Chung YJ, Barabote RD, Weyler W, Schilling CH, Saier MH, Jr. 2005. Catabolite repression and activation in *Bacillus subtilis*: dependency on CcpA, HPr, and HprK. J Bacteriol 187:7826–7839. https://doi.org/10.1128/JB.187.22.7826-7839.2005.
50. Yang Y, Zhang L, Huang H, Yang C, Yang S, Gu Y, Jiang W. 2017. A flexible binding site architecture provides new insights into CcpA global regulation in gram-positive bacteria. mBio 8:e02004-16. https://doi.org/10.1128/mBio.02004-16.
51. Marciniak BC, Pabijaniak M, de Jong A, Duhring R, Seidel G, Hillen W, Kuipers OP. 2012. High- and low-affinity *cre* boxes for CcpA binding in *Bacillus subtilis* revealed by genome-wide analysis. BMC Genomics 13:401. https://doi.org/10.1186/1471-2164-13-401.
52. Blencke HM, Homuth G, Ludwig H, Mader U, Hecker M, Stulke J. 2003. Transcriptional profiling of gene expression in response to glucose in *Bacillus subtilis*: regulation of the central metabolic pathways. Metab Eng 5:133–149. https://doi.org/10.1016/S1096-7176(03)00009-0.
53. Antunes A, Camiade E, Monot M, Courtois E, Barbut F, Sernova NV, Rodionov DA, Martin-Verstraete I, Dupuy B. 2012. Global transcriptional control by glucose and carbon regulator CcpA in *Clostridium difficile*. Nucleic Acids Res 40:10701–10718. https://doi.org/10.1093/nar/gks864.
54. Seidl K, Muller S, Francois P, Kriebitzsch C, Schrenzel J, Engelmann S, Bischoff M, Berger-Bachi B. 2009. Effect of a glucose impulse on the CcpA regulon in *Staphylococcus aureus*. BMC Microbiol 9:95. https://doi.org/10.1186/1471-2180-9-95.
55. Kim JH, Voskuil MI, Chambliss GH. 1998. NADP, corepressor for the Bacillus catabolite control protein CcpA. Proc Natl Acad Sci U S A 95:9590–9595. https://doi.org/10.1073/pnas.95.16.9590.
56. Danger JL, Cao TN, Cao TH, Sarkar P, Trevino J, Pflughoeft KJ, Sumby P. 2015. The small regulatory RNA FasX enhances group A Streptococcus virulence and inhibits pilus expression via serotype-specific targets. Mol Microbiol 96:249–262. https://doi.org/10.1111/mmi.12935.
57. Miller EW, Cao TN, Pflughoeft KJ, Sumby P. 2014. RNA-mediated regulation in Gram-positive pathogens: an overview punctuated with examples from the group A Streptococcus. Mol Microbiol 94:9–20. https://doi.org/10.1111/mmi.12742.
58. Pappesch R, Warnke P, Mikkat S, Normann J, Wisniewska-Kucper A, Huschka F, Wittmann M, Khani A, Schwengers O, Oehmcke-Hecht S, Hain T, Kreikemeyer B, Patenge N. 2017. The regulatory small RNA MarS supports virulence of *Streptococcus pyogenes*. Sci Rep 7:12241. https://doi.org/10.1038/s41598-017-12507-z.
59. Xu Y, Itzek A, Kreth J. 2014. Comparison of genes required for H_2O_2 resistance in *Streptococcus gordonii* and *Streptococcus sanguinis*. Microbiology 160:2627–2638. https://doi.org/10.1099/mic.0.082156-0.
60. Schumacher MA, Seidel G, Hillen W, Brennan RG. 2007. Structural mechanism for the fine-tuning of CcpA function by the small molecule effectors glucose 6-phosphate and fructose 1,6-bisphosphate. J Mol Biol 368:1042–1050. https://doi.org/10.1016/j.jmb.2007.02.054.
61. Ringquist S, Shinedling S, Barrick D, Green L, Binkley J, Stormo GD, Gold L. 1992. Translation initiation in *Escherichia coli*: sequences within the ribosome-binding site. Mol Microbiol 6:1219–1229. https://doi.org/10.1111/j.1365-2958.1992.tb01561.x.
62. Eriksen M, Sneppen K, Pedersen S, Mitarai N. 2017. Occlusion of the ribosome binding site connects the translational initiation frequency, mRNA stability and premature transcription termination. Front Microbiol 8:362. https://doi.org/10.3389/fmicb.2017.00362.
63. Ramsey MM, Rumbaugh KP, Whiteley M. 2011. Metabolite cross-feeding enhances virulence in a model polymicrobial infection. PLoS Pathog 7:e1002012. https://doi.org/10.1371/journal.ppat.1002012.
64. Pakula R, Walczak W. 1963. On the nature of competence of transformable streptococci. J Gen Microbiol 31:125–133. https://doi.org/10.1099/00221287-31-1-125.
65. Kawamura Y, Hou XG, Sultana F, Miura H, Ezaki T. 1995. Determination of 16S rRNA sequences of *Streptococcus mitis* and *Streptococcus gordonii* and phylogenetic relationships among members of the genus Strep-

tococcus. Int J Syst Bacteriol 45:406–408. https://doi.org/10.1099/00207713-45-2-406.
66. Yoshida Y, Ganguly S, Bush CA, Cisar JO. 2005. Carbohydrate engineering of the recognition motifs in streptococcal co-aggregation receptor polysaccharides. Mol Microbiol 58:244–256. https://doi.org/10.1111/j.1365-2958.2005.04820.x.
67. Cheng X, Redanz S, Cullin N, Zhou X, Xu X, Joshi V, Koley D, Merritt J, Kreth J. 2018. Plasticity of the pyruvate node modulates hydrogen peroxide production and acid tolerance in multiple oral streptococci. Appl Environ Microbiol 84:e01697-17. https://doi.org/10.1128/AEM.01697-17.
68. Dunny GM, Lee LN, LeBlanc DJ. 1991. Improved electroporation and cloning vector system for Gram-positive bacteria. Appl Environ Microbiol 57:1194–1201.
69. Podbielski A, Woischnik M, Leonard BA, Schmidt KH. 1999. Characterization of nra, a global negative regulator gene in group A streptococci. Mol Microbiol 31:1051–1064. https://doi.org/10.1046/j.1365-2958.1999.01241.x.
70. Sambrook J, Fritsch EF, Maniatis T. 1989. Molecular cloning: a laboratory manual, 2nd ed. Cold Spring Harbor Laboratory, Cold Spring Harbor, NY.
71. Loimaranta V, Tenovuo J, Koivisto L, Karp M. 1998. Generation of bioluminescent *Streptococcus mutans* and its usage in rapid analysis of the efficacy of antimicrobial compounds. Antimicrob Agents Chemother 42:1906–1910.
72. Zianni M, Tessanne K, Merighi M, Laguna R, Tabita FR. 2006. Identification of the DNA bases of a DNase I footprint by the use of dye primer sequencing on an automated capillary DNA analysis instrument. J Biomol Tech 17:103–113.
73. Edwards U, Rogall T, Blocker H, Emde M, Bottger EC. 1989. Isolation and direct complete nucleotide determination of entire genes. Characterization of a gene coding for 16S ribosomal RNA. Nucleic Acids Res 17:7843–7853.
74. Lane DJ (ed). 1991. 16S/23S rRNA sequencing. John Wiley & Sons, Chichester, United Kingdom.
75. Zbinden A, Kohler N, Bloemberg GV. 2011. recA-based PCR assay for accurate differentiation of *Streptococcus pneumoniae* from other viridans streptococci. J Clin Microbiol 49:523–527. https://doi.org/10.1128/JCM.01450-10.